

Syntheses, Structures, and Reactivities of Synthetic Analogues of the Three Forms of Co(III)–Bleomycin: Proposed Mode of Light-Induced DNA Damage by the Co(III) Chelate of the Drug

Jennifer D. Tan,[†] Samuel E. Hudson,[‡] Steven J. Brown,[‡] Marilyn M. Olmstead,[†] and Pradip K. Mascharak^{*‡}

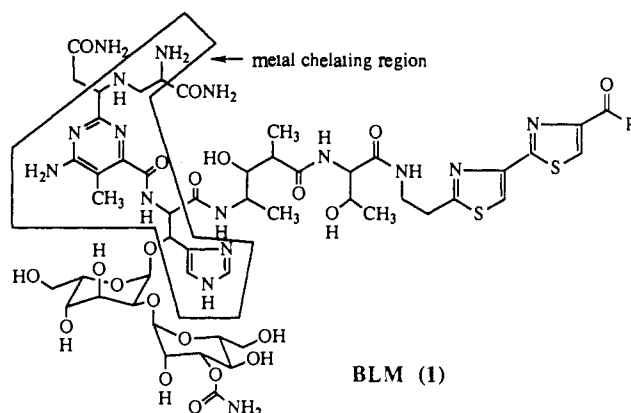
Contribution from the Department of Chemistry and Biochemistry, University of California, Santa Cruz, California 95064, and the Department of Chemistry, University of California, Davis, California 95616. Received July 29, 1991

Abstract: Three cobalt(III) complexes of a designed ligand PMAH, that mimics the metal-binding locus of the antitumor drug bleomycin (BLM), have been synthesized and structurally characterized. The complex [Co(PMA)(H₂O)](NO₃)₂ (**5**) crystallizes in the triclinic space group *P* $\bar{1}$ with *a* = 7.608 (3) Å, *b* = 10.542 (3) Å, *c* = 13.116 (4) Å, α = 71.14 (2)°, β = 74.59 (3)°, γ = 81.66 (3)°, *Z* = 2, and *V* = 957.7 (6) Å³. The complex [Co(PMA)(N-MeIm)](NO₃)₂·H₂O (**6**) also crystallizes in the triclinic space group *P* $\bar{1}$ with *a* = 8.485 (2) Å, *b* = 10.737 (3) Å, *c* = 15.080 (3) Å, α = 71.06 (2)°, β = 73.92 (2)°, γ = 69.94 (2)°, *Z* = 2, and *V* = 1199.3 (6) Å³. The third complex [Co(PMA)Cl]Cl·EtOH (**7**) crystallizes in the orthorhombic space group *Pbcn* with *a* = 13.228 (3) Å, *b* = 15.259 (4) Å, *c* = 21.287 (5) Å, *Z* = 8, and *V* = 4297 (2) Å³. In all three complexes, the deprotonated PMA[−] ligand binds the cobalt(III) center in a pentadentate fashion with five N donors situated in the pyrimidine and imidazole rings, primary and secondary amine groups, and the amide moiety. Only change in the sixth ligand (H₂O, N-MeIm, and Cl[−], respectively) gives rise to the brown (**5**), orange (**6**), and green (**7**) products. These complexes exhibit properties similar to the BROWN, ORANGE, and GREEN Co(III)–BLMs and therefore qualify as good models for the cobalt(III) chelates of the drug. For example, like Co(III)–BLMs, the present complexes **5–7** inflict strand breaks in DNA upon UV illumination and this photocleavage reaction does not require the presence of dioxygen. The light-induced DNA cleavage reaction by **5–7** is neither a consequence of photoreduction of the complexes to Co²⁺ nor are they initiated by singlet oxygen. Both DNA cleavage and spin-trapping experiments demonstrate that UV irradiation of **5–7** generates a C/N-based radical on the ligand framework which rapidly reacts with water to produce [•]OH radical. Since the positively-charged complexes bind DNA rather strongly, UV illumination results in rapid production of [•]OH radical in close proximity of the DNA helix with concomitant strand scission. A similar mechanism could account for the photocleavage of DNA by Co(III)–BLMs.

Introduction

The bleomycin (BLM, **1**) family of glycopeptide antibiotics is used in combination chemotherapy against several types of cancer.¹ These antibiotics require a metal ion like Fe²⁺ and molecular oxygen for their drug action.^{2–10} Oxidative damage of cellular DNA by the metal chelates of the drug (metallobleomycins, M–BLMs) is believed to be responsible for the antineoplastic activity. The requirement of dioxygen has been established firmly in case of iron- and copper-bleomycin.³ The DNA cleavage reaction is brought about by oxygen-based free radical(s) like [•]OH and/or hypervalent metal–oxo species formed in the vicinity of the DNA helix.^{2,3,11} In contrast, no oxygen activation of any kind has been noted with the kinetically inert (low-spin, d⁶) cobalt(III) complexes of BLM,¹² and despite strong binding to DNA, Co(III)–BLMs do not inflict damage to DNA under normal aerobic conditions. However, it has been recently reported that Co(III)–BLMs do cleave DNA when illuminated with UV^{13,14} or visible¹⁵ light, and this photoinduced DNA strand scission reaction is insensitive to dioxygen.¹⁶ This light-induced DNA degradation reaction of Co(III)–BLMs has raised renewed interest in the structures and photochemistry of the cobalt(III) complexes of BLM.

Aerobic oxidation of Co(II)–BLM¹⁷ affords several products.^{12,18–20} The first one is a short-lived BROWN mononuclear superoxo–Co(III) complex.^{17–19} Two molecules of brown Co–BLM react together with the loss of dioxygen to produce GREEN Co(III)–BLM which is predicted to be a dinuclear μ -peroxo complex.¹⁹ A report which contradicts this suggestion identifies a hydroperoxide (–OOH) group bound to cobalt in the GREEN form.²⁰ Another stable BROWN form with water as a ligand on cobalt is also reported.^{16,20} GREEN Co(III)–BLM is converted into ORANGE Co(III)–BLM on heating.¹² This thermodynamically stable orange form is reported to contain no “active”



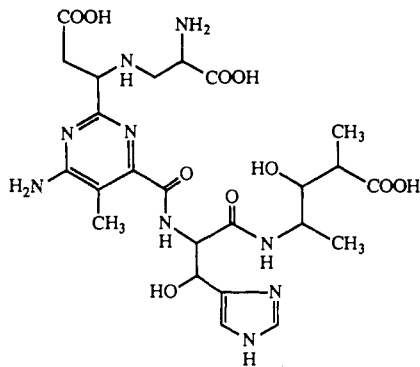
form of dioxygen in the coordination sphere of cobalt. Since hydrolysis of both GREEN and ORANGE Co(III)–BLM yield

- (1) Blum, R. H.; Carter, S. K.; Agre, K. A. *Cancer* **1973**, *31*, 903.
- (2) Petering, D. H.; Byrnes, R. W.; Antholine, W. E. *Chem.–Biol. Interact.* **1990**, *73*, 133.
- (3) Stubbe, J.; Kozarich, J. W. *Chem. Rev.* **1987**, *87*, 1107.
- (4) Hecht, S. M. *Acc. Chem. Res.* **1986**, *19*, 383.
- (5) Sugiura, T.; Takita, T.; Umezawa, H. *Met. Ions Biol. Syst.* **1985**, *19*, 81.
- (6) Dabrowiak, J. C. *Adv. Inorg. Biochem.* **1983**, *4*, 69.
- (7) Povrick, L. F. *Molecular Aspects of Anticancer Drug Action*; Neidle, S., Waring, M. J., Eds.; Macmillan: London, 1983; p 157.
- (8) Dabrowiak, J. C. *Met. Ions Biol. Syst.* **1980**, *11*, 305.
- (9) Umezawa, H.; Takita, T. *Struct. Bonding (Berlin)* **1980**, *40*, 73.
- (10) (a) *Bleomycin: Chemical, Biochemical and Biological Aspects*; Hecht, S. M., Ed.; Springer-Verlag: New York, 1979. (b) *Bleomycin: Current Status and New Developments*; Carter, S. K., Crooke, S. T., Umezawa, H., Eds.; Academic: New York, 1978.
- (11) Gajewski, E.; Aruoma, O. I.; Dizdaroğlu, M.; Halliwell, B. *Biochemistry* **1991**, *30*, 2444.
- (12) DeRiemer, L. H.; Mearns, C. F.; Goodwin, D. A.; Diamanti, C. I. *J. Med. Chem.* **1979**, *22*, 1019.

[†]University of California, Davis.

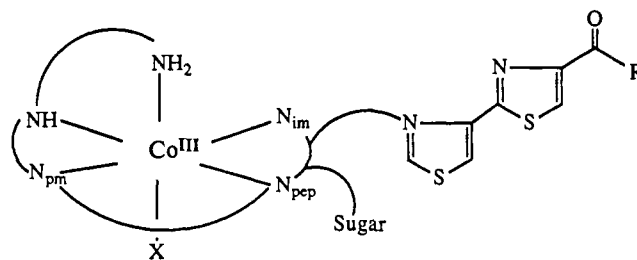
[‡]University of California, Santa Cruz.

the same cobalt(III) complex of pseudotetrapeptide A (**2**),²¹ it appears that the functional group of BLM which differentiates between the two Co(III)-BLMs is not a part of the tetrapeptide portion of the drug. Apart from the three *stable* aquo-BROWN, GREEN, and ORANGE Co(III)-BLMs, several Co(III)-BLMs with NO₂⁻, SCN⁻, and N₃⁻ as ligands have also been isolated by incubating the aquo-BROWN species with the appropriate ligand.²⁰ Also, in formate buffer, another brown formate-ligated Co(III)-BLM has been identified which reversibly interconverts to aquo-BROWN in aqueous solution.²⁰ Since studies on the DNA cleavage reactions have been restricted to the use of the aquo-BROWN, GREEN, and ORANGE Co(III)-BLMs,¹³⁻¹⁶ the present work is focussed on these three Co(III)-BLMs only.

Pseudotetrapeptide A (**2**)

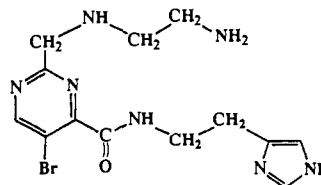
To date, no crystallographic information is available on any Co(III)-BLM. Comparison of spectral data of aquo-BROWN Co(III)-BLM^{16,20} and Co(III)-pseudotetrapeptide A²¹ reveals that in the former complex, BLM most probably employs five nitrogen donor centers located in the primary and secondary amines, pyrimidine ring and imidazole rings, and the peptide moiety next to the pyrimidine ring (the boxed area in **1**) to bind cobalt(III). The sixth coordination site is presumably occupied by a water molecule in both complexes. In ORANGE Co(III)-BLM, all six ligands to cobalt are believed to be supplied by BLM.¹⁶ The typical orange color suggests the presence of a CoN₆ chromophore. Further support comes from the fact that the electronic absorption spectrum of ORANGE Co(III)-BLM in the visible region is identical to that of NO₂-Co(III)-BLM²⁰ derived from aquo-BROWN and NO₂⁻. Similar chromatographic behavior and easy conversion to the orange form indicate that the coordination structure of GREEN Co(III)-BLM is very similar to that of the ORANGE Co(III)-BLM except for the presence of the -OOH group in the former. Since hydrolysis of both ORANGE and GREEN Co(III)-BLMs afford the same cobalt(III) complex of pseudotetrapeptide A, it is reasonable to assume that the three Co(III)-BLMs have the general structure **3** and differ from each other by one ligand only.

As part of our effort toward elucidation of the structures of M-BLMs and the mechanism(s) of DNA strand scission by the

**3**

X = H₂O , aquo-BROWN Co(III)-BLM
 X = -OOH , GREEN Co(III)-BLM
 X = N-donor , ORANGE Co(III)-BLM

metallo-drugs, we have synthesized a designed ligand PMAH (**4**, H is the dissociable amide H) which resembles the metal-chelating portion of BLM (boxed area in **1**) very closely. Isolation and structure determination of the copper(II) complex of **4**, namely [Cu(II)-PMA]⁺, have established the structure of Cu(II)-BLM at physiological pH.^{23,24} Results of the spin-trapping and DNA cleavage reactions by [Cu(II)-PMA]X (X = ClO₄⁻, BF₄⁻)²⁵ have indicated that (a) both Cu(II)-BLM and [Cu(II)-PMA]⁺ inflict strand breaks in double-stranded DNA in the presence of suitable concentration of a reductant and oxygen and (b) the DNA strand scission is brought about by [•]OH radical formed in a copper-driven Fenton-like reaction.²⁶ Since DNA cleavage by Co(III)-BLMs is induced by light and *not* dependent on the concentration of dissolved oxygen,¹⁶ the mechanism of strand scission is different. We therefore decided to (a) synthesize good models for the three stable forms of Co(III)-BLM, (b) explore the photochemistry of the model complexes, and (c) study the photoinduced DNA cleavage reactions by the model compounds to figure out the mechanism(s) of the intriguing reaction(s). Reported here are the syntheses and structures of three cobalt(III) complexes of PMAH, namely [Co(PMA)(H₂O)]X₂ (X = NO₃⁻, ClO₄⁻) (**5**), [Co(PMA)(N-MeIm)](NO₃)₂·H₂O (N-MeIm = *N*-methylimidazole, **6**), and [Co(PMA)Cl]Cl·EtOH (**7**), which are good models for the BROWN, ORANGE, and GREEN Co(III)-BLM, respectively. The spectroscopic properties of these synthetic analogues²⁷ have been compared carefully with those of the respective Co(III)-BLMs in order to establish the coordination structures of the different Co(III)-BLMs. Also reported are the results of DNA cleavage by these analogues under conditions that are reported for the Co(III)-BLMs.¹³⁻¹⁶ Results from the DNA cleavage reactions and spin trapping experiments in aqueous and nonaqueous media have provided a mechanism for the light-driven DNA strand scission reactions by the analogues **5-7**. Similarities in spectral parameters as well as the characteristics of the DNA cleavage reaction by the analogues and the Co(III)-BLMs suggest that the same mechanism could account for the observed photoactivity of the Co(III)-BLMs. Part of this work, namely the synthesis, structure, and DNA cleavage capacity of **5** has been the subject of a previous communication from this laboratory.²⁸

PMAH (**4**)

(13) Saito, I.; Morii, T.; Sugiyama, H.; Matsuura, T.; Meares, C. F.; Hecht, S. M. *J. Am. Chem. Soc.* **1989**, *111*, 2307. (b) Chang, C.-H.; Meares, C. F. *Biochemistry* **1982**, *21*, 6332.

(14) (a) Suzuki, T.; Kuwahara, J.; Goto, M.; Sugiura, Y. *Biochim. Biophys. Acta* **1985**, *824*, 330. (b) Suzuki, T.; Kuwahara, J.; Sugiura, Y. *Nucl. Acids Res.* **1984**, *15*, 161.

(15) Subramanian, R.; Meares, C. F. *J. Am. Chem. Soc.* **1986**, *108*, 6427.

(16) Chang, C.-H.; Meares, C. F. *Biochemistry* **1984**, *23*, 2268.

(17) Sugiura, Y. *J. Am. Chem. Soc.* **1980**, *102*, 5216.

(18) (a) Vos, C. M.; Westera, G. *J. Inorg. Biochem.* **1981**, *15*, 253. (b)

Vos, C. M.; Westera, G.; Schipper, D. *J. Inorg. Biochem.* **1980**, *13*, 165. (c)

Vos, C. M.; Westera, G.; van Zanten, B. *J. Inorg. Biochem.* **1980**, *12*, 45.

(19) (a) Albertini, J. P.; Garnier-Suillerot, A. *Biochemistry* **1982**, *21*, 6777.

(b) Garnier-Suillerot, A.; Albertini, J. P.; Tosi, L. *Biochem. Biophys. Res. Commun.* **1981**, *102*, 499.

(20) Chang, C.-H.; Meares, C. F. *Biochem. Biophys. Res. Commun.* **1983**, *110*, 959.

(21) (a) Dabrowiak, J. C.; Tsukayama, M. *J. Am. Chem. Soc.* **1981**, *103*, 7543. (b) Pseudotetrapeptide A is a hydrolysis product of BLM that lacks both the bithiazole and the sugar moieties of the drug.

(22) The same coordination structure has also been proposed for the cobalt(III) complex of pseudotetrapeptide A.²¹

(23) Brown, S. J.; Stephan, D. W.; Mascharak, P. K. *J. Am. Chem. Soc.* **1988**, *110*, 1996.

(24) Brown, S. J.; Hudson, S. E.; Stephan, D. W.; Mascharak, P. K. *Inorg. Chem.* **1989**, *28*, 468.

(25) Hudson, S. E.; Mascharak, P. K. *Chem. Res. Toxicol.* **1989**, *2*, 411.

(26) Sigman, D. S. *Acc. Chem. Res.* **1986**, *19*, 180.

(27) Ibers, J. A.; Holm, R. H. *Science (Washington, D.C.)* **1980**, *209*, 223.

(28) Brown, S. J.; Hudson, S. E.; Olmstead, M. M.; Mascharak, P. K. *J. Am. Chem. Soc.* **1989**, *111*, 6446.

Table I. Summary of Crystal Data, Intensity Collection, and Structure Refinement Parameters^a for [Co(PMA)(H₂O)](NO₃)₂ (**5**), [Co(PMA)(N-Melm)](NO₃)₂·H₂O (**6**), and [Co(PMA)Cl]Cl·EtOH (**7**)

	5	6	7
formula (mol wt)	CoC ₁₃ H ₁₉ N ₉ O ₈ Br (568.19)	CoC ₁₇ H ₂₅ N ₁₁ O ₈ Br (650.32)	CoC ₁₅ H ₂₃ N ₇ O ₂ BrCl ₂ (543.22)
color and habit	red blocks	orange-red plates	reddish green prisms
crystal system	triclinic	triclinic	orthorhombic
space group	<i>P</i> $\bar{1}$	<i>P</i> $\bar{1}$	<i>Pbcn</i>
<i>a</i> , Å	7.608 (3)	8.485 (2)	13.228 (3)
<i>b</i> , Å	10.542 (3)	10.737 (3)	15.259 (4)
<i>c</i> , Å	13.116 (4)	15.080 (3)	21.287 (5)
α , deg	71.14 (2)	71.06 (2)	
β , deg	74.59 (3)	73.92 (2)	
γ , deg	81.66 (3)	69.94 (2)	
<i>Z</i>	2	2	8
<i>V</i> , Å ³	957.7 (6)	1199.3 (6)	4297 (2)
<i>d</i> _{calcd} , g/cm ³	1.97	1.80	1.68
abs coeff (μ), cm ⁻¹	30.25	24.29	29.15
range of trans factors	0.65–0.88	0.56–0.78	0.55–0.69
scan method	ω , 1° range 1.8° offset for bkgnd	ω , 0.9° range 0.9° offset for bkgnd	ω , 1.1° range
scan speed, deg min ⁻¹	8	8	8
2 θ range, deg	0–50	0–50	0–50
octants colled	<i>h, ±k, ±l</i>	<i>h, ±k, ±l</i>	<i>h, k, l</i>
no. of data colled	3381	4161	4243
no. of data used in refinement	2648 [<i>I</i> > 2 σ (<i>I</i>)]	3623 [<i>I</i> > 2 σ (<i>I</i>)]	2729 [<i>I</i> > 2 σ (<i>I</i>)]
no. of parameters refined	289	370	253
<i>R</i> ^b	0.049	0.031	0.052
<i>R</i> _w ^c	0.053	0.034	0.049

^a Radiation (λ , Å); Mo K α (0.71069); *T*, 130 K. ^b $R = \sum ||F_o| - |F_c|| / |F_o|$. ^c $R_w = \sum ||F_o| - |F_c|| w^{1/2} / \sum |F_o| w^{1/2}$.

Experimental Section

Preparation of Compounds. PMAH and Na₃[Co(CO₃)₃]:3H₂O were synthesized by following the published procedures.^{23,29} 1-Methylimidazole and 5,5-dimethyl-1-pyrroline-*N*-oxide (DMPO) were procured from Aldrich Chemical Co. The strongly acidic cation exchanger SP-C50-120 and bovine erythrocyte superoxide dismutase (SOD) were purchased from Sigma Chemical Co. Chelex 100 resin, ethidium bromide, and plasmid DNA ϕ X174 (RF) were obtained from the Bio-Rad laboratories, Fluka Chemie, and the Bethesda Research Laboratories (BRL), respectively. Bleomycin was a gift from the Cetus Corporation, and the Co(III)-BLMs were synthesized by following the procedure of DeRiemer et al.¹²

[Co(PMA)(H₂O)](NO₃)₂ (5**).** A slurry of 570 mg (1.6 mmol) of Na₃[Co(CO₃)₃]:3H₂O and 700 mg (1.9 mmol) of PMAH in 10 mL of water was stirred at room temperature for 3 h. The pH of the reaction mixture was maintained at 5 with 0.5 N HBF₄.³⁰ The deep red solution thus obtained was loaded on a SP-C50-120 Sephadex column (6 × 20 cm) and eluted with 0.1 N aqueous KCl solution. The first band was collected and evaporated to dryness, and the excess KCl was removed by extracting the residue with ethanol. The green ethanolic extract on evaporation afforded a green solid which was washed with 3 × 10 mL of acetonitrile to remove a blue-green impurity. A batch of 500 mg of green solid that analyzes as [Co(PMA)Cl₂·HCl]²⁸ was obtained. Next, the green solid was dissolved in 5 mL of water, and to the orange-brown solution was added a solution of 480 mg (2.8 mmol) of AgNO₃ in 5 mL of water. The mixture was stirred vigorously at 50 °C for 10 min, and the precipitate of AgCl was filtered off. The orange filtrate was then stored at room temperature for 3 h and filtered once again to remove traces of AgCl. The filtrate was evaporated to dryness under reduced pressure. The reddish brown residue was dissolved in 10 mL of aqueous methanol (1:1) and to it was added 300 mg of LiNO₃. Slow evaporation of this solution afforded reddish brown blocks of **5** (yield 25% based on Na₃[Co(CO₃)₃]:3H₂O): Selected IR bands (KBr pellet, cm⁻¹) 3126 (m, br), 2910, 1618 (vs, ν_{CO}), 1560 (s), 1510, 1440 (s), 1380 (vs, $\nu(NO_3^-)$), 1220 (m), 1095, 1040 (w), 828 (m), 773 (m), 703 (m), 627 (w). Anal. Calcd for CoC₁₃H₁₉N₉O₈Br: C, 27.46; H, 3.37; N, 22.19. Found: C, 27.40; H, 3.29; N, 22.24. The perchlorate salt [Co(PMA)(H₂O)](ClO₄)₂ was synthesized by using LiClO₄ instead of LiNO₃.

[Co(PMA)(N-Melm)](NO₃)₂·H₂O (6**).** A solution of 90 mg of **5** (0.16 mmol) in 10 mL of (CH₃)₂SO³² was heated at 90 °C for 1 h. The solvent

was then removed under vacuum, and the brown residue was redissolved in 10 mL of (CH₃)₂SO together with 40 μ L (0.5 mmol) of *N*-methylimidazole (*N*-Melm). This mixture was heated at 90 °C for 2 h. Again the solvent was removed under vacuum. Next, the orange-brown residue was dissolved in 5 mL of water, and the solution was loaded on a SP-C50-120 Sephadex column (3 × 15 cm) and eluted with 0.05 N aqueous KCl solution. The first orange band was collected, and a workup similar to the one described above afforded 45 mg (48%) of shiny orange plates. This product was dissolved in 10 mL of ethanol together with 100 mg of LiNO₃, and the resulting orange solution was stored at room temperature for 4 days. Orange plates of **6** thus separated were collected by filtration: Selected IR bands (KBr pellet, cm⁻¹) 3423 (s, br), 3120 (s, br), 1618 (s, ν_{CO}), 1560 (s), 1384 (vs, $\nu(NO_3^-)$), 1243 (w), 1220 (m), 1095 (s), 825 (w), 756 (m), 703 (m), 688 (m), 620 (m). Anal. Calcd for CoC₁₇H₂₅N₁₁O₈Br: C, 31.38; H, 3.87; N, 23.70. Found: C, 31.47; H, 3.81; N, 23.29.

[Co(PMA)Cl]Cl·EtOH (7**).** A slurry of 615 mg (1.7 mmol) of Na₃[Co(CO₃)₃]:3H₂O and 750 mg (2.04 mmol) of PMAH in 10 mL of water was stirred at room temperature for 3 h. The pH of the reaction mixture was kept around 5 with 0.5 N HBF₄ during this period. The resulting deep red solution was loaded on a SP-C50-120 Sephadex column (6 × 20 cm) and eluted with 0.1 N aqueous KCl solution. The first band was collected, evaporated to dryness and desalted by extracting into ethanol. The green filtrate on evaporation afforded a green residue which was washed with 3 × 10 mL of acetonitrile to remove a blue-green impurity. A batch of 675 mg of green powder was obtained. Further purification of the product was achieved by passing it through another SP-C50-120 Sephadex column (3 × 10 cm) with 0.05 N aqueous KCl solution as the eluent. The first green band was collected and worked up as described above. The light-green product (225 mg) was dissolved in anhydrous ethanol, and the solution was stored over H₂SO₄ in a desiccator. The yield of [Co(PMA)Cl]Cl·EtOH (**7**) was 25% based on Na₃[Co(CO₃)₃]:3H₂O: Selected IR bands (KBr pellet, cm⁻¹) 3072 (s), 2890 (s), 1626 (vs, ν_{CO}), 1553 (m), 1442 (w), 1345 (m), 1222 (m), 1095 (m), 1042 (m), 818 (w), 686 (m), 625 (m). Anal. Calcd for CoC₁₅H₂₃N₇O₂BrCl₂: C, 33.15; H, 4.27; N, 18.06. Found: C, 32.98; H, 4.15; N, 18.11.

X-ray Data Collection, Structure Solution, and Refinement. Crystals of **5** and **6** were obtained by slow evaporation (in air) of solutions of the complexes in water and ethanol, respectively. In case of **7**, evaporation of the ethanolic solution was carried out in a desiccator with H₂SO₄ as the desiccant. Diffraction data were collected at 130 K on either a Synthex P2₁ or a Siemens R3m/V machine, both of which were equipped with graphite monochromator and modified LT-1 low temperature apparatus. Mo K α radiation ($\lambda = 0.71069$ Å) was employed. Only random fluctuations of <2% in the intensities of three standard reflections were

(29) Bauer, H. F.; Drinkard, W. C. *Inorg. Synth.* 1966, 8, 202.

(30) If the pH of the otherwise basic mixture is not adjusted with HBF₄, the imidazole moiety of PMAH is deprotonated, and this results in formation of imidazole-bridged tri- and tetrameric cobalt(III) complexes of PMAH₂H (both peptide H and imidazole H lost). These complexes have been isolated and structurally characterized.³¹

(31) Brown, S. J.; Olmstead, M. M.; Mascharak, P. K. *Inorg. Chem.* 1989, 28, 3720.

(32) *N,N*-Dimethylformamide (DMF) can be used in place of (CH₃)₂SO (DMSO) in this synthesis.

observed during the courses of data collection.

The structures of **5** and **6** were solved by Patterson methods.^{33,34} Hydrogen atoms bonded to the carbon atoms were included at calculated positions using a riding model, with C-H = 0.96 Å and $U_H = 1.2U_C$. An absorption correction was applied to both data sets.³⁵ In case of **5**, non-hydrogen atoms were assigned anisotropic thermal parameters in the final cycles of refinement.³⁶ The largest feature on a final difference map was 1.29 eÅ⁻³ in height, 1.09 Å from Br. The hydrogen atoms on the water molecule bonded to Co were located on a final difference map but were not refined. With **6**, in the final cycles of refinement, non-hydrogen atoms were refined anisotropically. The hydrogen atoms bonded to lattice water and the nitrogen atoms of the complex cation were located on a difference map and allowed to refine. The largest feature on a final difference map was 0.61 eÅ⁻³ in height.

Systematic absences $0kl$ ($k = 2n + 1$), $h0l$ ($l = 2n + 1$), and hko ($h + k = 2n + 1$) in the data set for **7** are consistent with the orthorhombic space group *Pbcn*. The structure was solved by direct methods.³⁷ In the final cycles of refinement, non-hydrogen atoms were assigned anisotropic thermal parameters. For the hydrogen atoms bonded to carbon atoms, the riding model was used with fixed isotropic *U* values. The data were corrected for absorption effects.³⁵ The largest feature on a final difference map was 1.05 eÅ⁻³ in height.

Machine parameters, crystal data, and data collection parameters for **5-7** are summarized in Table I. Selected bond distances and angles are listed in Table II. The following data for **5-7** have been submitted as supplementary material: atomic coordinates and isotropic thermal parameters for the non-hydrogen atoms (Tables S1-S3), complete lists of bond distances (Tables S4-S6) and angles (S7-S9), anisotropic thermal parameters (Tables S10-S12), H atom coordinates (Tables S13-S15), and values of $|0F_o|$ and $|0F_c|$ (Tables S16-S18).

Other Physical Measurements. Infrared spectra were obtained with a Perkin-Elmer 1600 FTIR spectrometer. Absorption spectra were measured on a Perkin Elmer Lambda 9 spectrophotometer. ¹H and ¹³C NMR spectra were recorded on a General Electric 300-MHz GN-300 instrument. Samples were dissolved in (CD₃)₂SO (99.5% D). Multiplicities of ¹³C NMR peaks were determined from APT and DEPT data.³⁸ Standard pulse sequences³⁹ were used to obtain ¹H-¹H and ¹H-¹³C two-dimensional scalar-correlated NMR spectra. The experimental details have already been published.⁴⁰ The spin-trapping experiments (20 °C) were performed at X-band frequencies by using a Bruker ESP-300 spectrometer. 5,5-Dimethyl-1-pyrroline-*N*-oxide (DMPO) was used as the spin trap. Agarose gel (1%) electrophoreses were run on BRL H-5 horizontal gel system. Photographs were taken with a Polaroid MP-4 system following ethidium bromide staining. Densitometry of DNA cleavage products on the gels was carried out with a BioRad Model 620 video Densitometer interfaced with a Compaq 386/20e computer.

Solutions. The DNA cleavage reactions were carried out in Tris-borate buffer (25 mM) with 190 μM EDTA, pH 8.0. The glasswares were acid-washed and rinsed with deionized distilled water. All solutions were passed through Chelex 100 column prior to use. DMPO was purified according to literature procedure.⁴¹ The nonaqueous solvents were purified by distillation following storage over suitable drying agents.

DNA Cleavage Experiments. Reaction mixtures (40 μL total volume) contained 1.6 μg of ϕ X174 (RF) DNA in 25 mM Tris-borate buffer. The samples were placed into a multiple-well tissue culture cluster plate (volume of the well = 90 μL) and covered with a quartz plate and a 320 nm filter (Corning 5950).⁴² A transilluminator (UVP-TM-36, $\lambda_{max} = 302$ nm, intensity 7 mW/cm²) was placed face-down over the plate. The distance between the light source and the samples was 4 cm. At the end of the illumination time, the samples were diluted with equivalent amounts of dye and loaded onto 1% aqueous gel (running buffer Tris-

acetate 40 mM, 1 mM EDTA, pH 8) and electrophoresed for 3 h at 100 V.

Spin-Trapping Experiments. The spin adducts of DMPO were generated as follows. Thoroughly degassed aqueous solution of DMPO and TBE buffer (freeze-thaw method under dynamic vacuum) and tared amounts of the cobalt complexes were taken inside a glovebox. The solutions were prepared under a pure dinitrogen atmosphere, mixed together, and transferred into quartz cuvettes which were sealed with Teflon stoppers and Parafilm. These were then irradiated as in the DNA cleavage experiments. Once the irradiation time was over, the contents were immediately transferred to capillary tubes under dinitrogen and their ESR spectra recorded.

Mixtures in nonaqueous solvents were prepared and illuminated in a similar manner. In all cases, proper blanks were subjected to ESR measurements to ensure that the ESR-active species were indeed produced from the cobalt complexes and not from the irradiated spin trap, buffer chemicals or solvents.

Detection of Co²⁺. That the present Co(III) complexes **5-7** are not photoreduced under the experimental conditions of the DNA cleavage reactions as well as the spin trapping experiments were checked by the published analytical procedure.⁴³ Mixtures of millimolar solutions of the cobalt complexes and 0.36 M KSCN were irradiated at 320 nm for 1 h. An equal volume of acetone was added, and the intensity of the 620 nm band (if any) was measured. This procedure afforded satisfactory results with [Co(NH₃)₆]Cl₃ which is known to release Co²⁺ ion in aqueous solution as a result of photoreduction.

Results and Discussion

Co(III) complexes are usually synthesized by aerobic (or chemical) oxidation of mixtures of Co(II) salts and the appropriate ligands. These reactions often proceed via μ -peroxo or μ -oxo binuclear intermediates.⁴⁴ The Co(III)-BLMs have been synthesized by this conventional route,¹² and both brown μ -peroxo¹⁹ and green species with -OOH group bonded to cobalt²⁰ have been reported. In the present work, aerobic oxidation of mixtures of Co(II) salts and PMAH produced brown solutions indicating the presence of cobalt-oxo species. However, all attempts to isolate crystalline solid(s) from these mixtures failed. Following several unsuccessful attempts, the alternative method of ligand substitution with the convenient Co(III) starting material Na₃[Co(CO₃)₃]·3H₂O and PMAH was tried.⁴⁵ Addition of PMAH to a slurry of Na₃[Co(CO₃)₃]·3H₂O in water indeed resulted in a rapid color change of green to orange-red. However, careful workup of the orange solution including passage through a SP-C50-120 Sephadex column afforded imidazolate-bridged trimeric and tetrameric complexes.³¹ These multinuclear Co(III) complexes of the doubly-deprotonated PMAH²⁻ form quite rapidly since (a) Co(III) almost exclusively prefers six-coordination and PMAH offers a maximum of five donor centers to one metal ion and (b) the basicity of the initial reaction mixture causes deprotonation of the NH group of the imidazole moiety⁴⁶⁻⁴⁸ and allows bridge formation between coordinatively unsaturated Co(III) centers by the imidazolate group. Once the role of pH in this reaction was realized, we were able to isolate the desired mononuclear [Co(PMA)L]ⁿ⁺ (L = H₂O or N-Melm, $n = 2$; L = Cl⁻, $n = 1$) complexes by maintaining the pH of the reaction mixture close to 5 by addition of aliquots of HBF₄ throughout the entire period of mixing. This pH is apparently sufficient to allow deprotonation of the amide function of PMAH but not the imidazole NH group.

(33) SHELXTL, Revision 5.1 programs, installed on a Data General Eclipse computer.

(34) Neutral atom scattering factors and corrections for anomalous dispersion were taken from *International Tables for X-ray Crystallography*; Kynoch Press: Birmingham, England, 1974; Vol. IV.

(35) The absorption correction was made by use of the program XABS; Moezzi, B. Ph.D. Dissertation, University of California, Davis, 1987. The program obtains an absorption tensor from $F_o - F_c$ differences.

(36) In all three cases, full-matrix least-squares techniques were employed.

(37) SHELXTL PLUS (VMS), installed on a Micro VAX 3200 computer.

(38) Patt, S. L.; Shoolery, J. N. *J. Magn. Reson.* **1982**, *46*, 535.

(39) Bunn, R.; Gunther, H. *Angew. Chem., Int. Ed. Engl.* **1983**, *48*, 350.

(40) Delany, K.; Arora, S. K.; Mascharak, P. K. *Inorg. Chem.* **1988**, *27*, 705.

(41) Buettner, G. R. In *CRC Handbook of Methods for Oxygen Radical Research*; Greenwald, R. A., Ed.; CRC Press: Boca Raton, FL, 1985; p 151.

(42) The filter blocks the high energy (270-300 nm) UV light and prevents excitation and/or generic photolytic damage of DNA and the spin trap.

(43) Hughes, R. G.; Endicott, J. F.; Hoffman, M. Z.; House, D. A. *J. Chem. Ed.* **1969**, *46*, 440.

(44) Cotton, F. A.; Wilkinson, G. In *Advanced Inorganic Chemistry*, 5th ed.; Wiley: New York, 1988; pp 735-738.

(45) The green tris(carbonato)cobaltate(III) anion is often used as the Co(III) starting material since substitution of the carbonate groups can be easily controlled by the kind and amount of the incoming ligand and by temperature, pH, and other parameters. For more examples, see: Shibata, M. *Top. Curr. Chem.* **1983**, *110*, 26.

(46) The pK_a of the NH group of imidazole coordinated to Co(III) has been estimated to be close to 11.⁴⁷

(47) (a) Harrowfield, J. M.; Norris, V.; Sargeson, A. M. *J. Am. Chem. Soc.* **1976**, *98*, 7282. (b) Brodsky, N. R.; Nguyen, N. W.; Rowan, N. S.; Storm, C. B.; Butcher, R. J.; Sinn, E. *Inorg. Chem.* **1984**, *23*, 891.

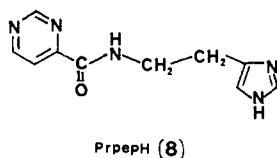
(48) For more examples of imidazolate-bridged Co(III) complexes see: (a) Hawkins, C. J.; Horn, E.; Martin, J.; Palmer, J. A. L.; Snow, M. R. *Aust. J. Chem.* **1986**, *39*, 1213. (b) Morris, P. J.; Martin, R. B. *J. Inorg. Nucl. Chem.* **1971**, *33*, 2913.

The major product⁴⁹ in the orange-red solution from the $\text{Na}_3[\text{Co}(\text{CO}_3)_3] \cdot 3\text{H}_2\text{O}/\text{PMAH}$ reaction is presumably the aquo complex $[\text{Co}(\text{PMA})(\text{H}_2\text{O})]^{2+}$ (or a variation thereof) which is converted into the chloro complex $[\text{Co}(\text{PMA})\text{Cl}]^+$ while passing through the Sephadex column containing a large excess of Cl^- . Indeed, the material eluted from the column dissolves in ethanol to give a green solution. This product, on another passage through a Sephadex column, affords pure 7. On long standing in aqueous solution 7 is converted into 5. An alternative (and faster) to this aqueous reaction is to allow 7 to react with AgNO_3 , a reaction which generates 5 in almost quantitative yield. The H_2O ligand in 5 can be easily replaced by DMSO by heating a solution of 5 in the latter solvent. Replacement of H_2O by DMSO can be followed by NMR (vide infra) or UV-vis absorption spectroscopy (color changes from orange-brown to greenish-brown).

The DMSO adduct $[\text{Co}(\text{PMA})(\text{DMSO})]^{2+}$ is a convenient starting material for other $[\text{Co}(\text{PMA})\text{L}]^{n+}$ complexes since DMSO can be easily replaced by other ligands like N-MeIm. In the present work, synthesis of $[\text{Co}(\text{PMA})(\text{N-MeIm})]^{2+}$ has been accomplished via $[\text{Co}(\text{PMA})(\text{DMSO})]^{2+}$ instead of $[\text{Co}(\text{PMA})(\text{H}_2\text{O})]^{2+}$ for this reason.

Structure of $[\text{Co}(\text{PMA})(\text{H}_2\text{O})(\text{NO}_3)_2]$ (5). The structure consists of discrete cations and anions. A computer-generated drawing of the cation is shown in Figure 1, and selected bond distances and angles are listed in Table II. The coordination geometry around cobalt is octahedral. Four nitrogens from the pyrimidine, imidazole, secondary amine, and the deprotonated amide group of the ligand form the basal plane of coordination, while the primary amine and the water molecule occupy the axial positions. The ligand is thus anionic (PMA^-) and pentadentate. This mode of coordination of PMA^- to cobalt is retained in all three complexes 5-7.

The Co(III)-N distances in 5 range from 1.865 (4) to 2.004 (4) Å and are comparable to those found in related compounds.^{31,40,50} For example, in the "bis" complex of Co(III) with the ligand PrpepH (8, H stands for the dissociable amide H), namely, $[\text{Co}(\text{Prpep})_2]\text{ClO}_4 \cdot 2.25\text{H}_2\text{O}$ (9), the Co(III)- N_{pm} (pm = pyrimidine), Co(III)- N_{im} (im = imidazole), and Co(III)-N (amido) bonds are, respectively, 1.943 (5), 1.931 (5), and 1.927 (5) Å long.⁵⁰ In 5, the corresponding distances are 1.865 (4), 1.912 (5), and 1.917 (4) Å, respectively. Additional comparative



data could be found in ref 50. The Co(III)- NH_2 and Co(III)-NH bond lengths in 5 fall within the range (1.85-2.10 Å) noted for various trimethylenetetramine⁵¹ and tetraethylenepentamine⁵² complexes of trivalent cobalt. The Co(III)-O(2) bond distance (1.945 (4) Å) is similar to the Co(III)- OH_2 distances observed in Co(III) complexes containing coordinated H_2O molecule(s) (range 1.94-1.97 Å).⁵³ In the ligand framework, minor lengthening of the peptide carbonyl bond (1.240 (6) Å) is noted as a result of coordination of the deprotonated amido N to cobalt.^{54,55} Metric parameters of the pyrimidine as well as the

(49) A deep brown band is always left on the Sephadex column which could be taken out only with 2 M aqueous KCl solution. The product(s) present in this band has not been characterized.

(50) Muetterties, M.; Cox, M. B.; Arora, S. K.; Mascharak, P. K. *Inorg. Chim. Acta* 1989, 160, 123.

(51) Freeman, H. C.; Maxwell, I. E. *Inorg. Chem.* 1970, 9, 649. (b) Freeman, H. C.; Marzilli, L. G.; Maxwell, I. E. *Inorg. Chem.* 1970, 9, 2408. (c) Buckingham, D. A.; Maxwell, I. E.; Sargeson, A. M.; Snow, M. R. *J. Am. Chem. Soc.* 1970, 92, 3617. (d) Buckingham, D. A.; Marzilli, L. G.; Sargeson, A. M.; Turnbull, K. R. *J. Am. Chem. Soc.* 1974, 96, 1713.

(52) (a) Snow, M. R. *J. Chem. Soc., Dalton Trans.* 1972, 1627. (b) Snow, M. R. *J. Am. Chem. Soc.* 1970, 92, 3610.

(53) (a) Kanazawa, Y.; Matsumoto, T. *Acta Crystallogr.* 1976, B32, 282. (b) Freeman, H. C.; Maxwell, I. E. *Inorg. Chem.* 1969, 8, 1293.

(54) Sigel, H.; Martin, R. B. *Chem. Rev.* 1982, 82, 385.

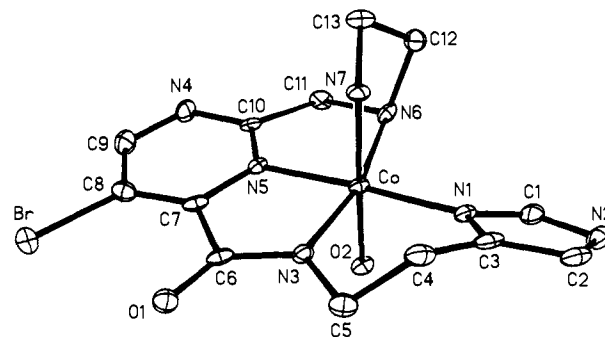


Figure 1. Thermal ellipsoid (probability level 50%) plot of $[\text{Co}(\text{PMA})(\text{H}_2\text{O})]^{2+}$ (cation of 1) with the atom-labeling scheme. Hydrogen atoms are omitted for the sake of clarity.

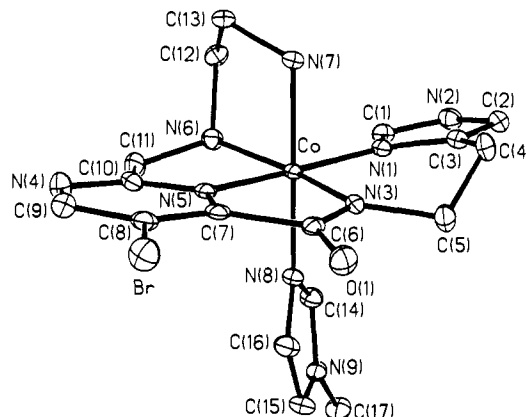


Figure 2. Thermal ellipsoid (probability level 50%) plot of $[\text{Co}(\text{PMA})(\text{N-MeIm})]^{2+}$ (cation of 2) with the atom-labeling scheme. Hydrogen atoms are omitted for the sake of clarity.

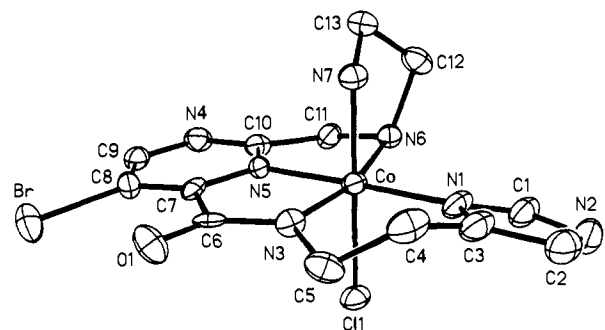


Figure 3. Thermal ellipsoid (probability level 50%) plot of $[\text{Co}(\text{PMA})\text{Cl}]^+$ (cation of 3) with the atom-labeling scheme. Hydrogen atoms are omitted for the sake of clarity.

imidazole ring are unexceptional.

In 5, significant deviations from 90° are observed with the N-Co-N angles in the five-membered chelate rings (Table II). The remaining angles are close to 90° , however. The pyrimidine ring, the $-\text{CH}_2\text{NH}-$ moiety, and the peptide group all lie on a plane. The dihedral angle between this plane (containing N(3), N(4), N(5), N(6), C(6), C(7), C(8), C(9), C(10), and C(11), designated as plane 1 hereafter) and the plane of the imidazole ring (containing N(1), N(2), C(1), C(2), and C(3)) is 26.6° . The two CH_2 groups (C(4) and C(5)) connecting the peptide function and the imidazole ring lie above and below the mean basal plane (Figure 1).

Structure of $[\text{Co}(\text{PMA})(\text{N-MeIm})(\text{NO}_3)_2 \cdot \text{H}_2\text{O}$ (6). The structure of the cation is illustrated in Figure 2, and selected bond distances and angles are included in Table II. The lattice water molecule is H-bonded to the peptide oxygen (O(8)-O(1) = 2.799 (3) Å). Additional H-bonding interactions are evident among

(55) This feature is real and present in all the three structures. Shift of ν_{CO} to lower energy (ca. 40 cm^{-1}) is also noted in the IR spectra.

Table II. Selected Bond Distances (Å) and Angles (deg) for 5-7

bond distances				bond angles			
[Co(PMA)(H ₂ O)](NO ₃) ₂ (5)							
Co-O(2)	1.945 (4)	Co-N(1)	1.912 (5)	O(2)-Co-N(1)	91.5 (2)	O(2)-Co-N(3)	92.5 (2)
Co-N(3)	1.917 (4)	Co-N(5)	1.865 (4)	N(1)-Co-N(3)	93.4 (2)	O(2)-Co-N(5)	88.0 (2)
Co-N(6)	2.004 (4)	Co-N(7)	1.933 (5)	N(1)-Co-N(5)	175.7 (2)	N(3)-Co-N(5)	82.4 (2)
O(1)-C(6)	1.240 (6)	N(1)-C(1)	1.335 (8)	O(2)-Co-N(6)	89.7 (2)	N(1)-Co-N(6)	100.4 (2)
N(1)-C(3)	1.399 (6)	N(3)-C(5)	1.465 (7)	N(3)-Co-N(6)	166.1 (2)	N(5)-Co-N(6)	83.9 (2)
N(3)-C(6)	1.338 (7)	N(4)-C(10)	1.335 (7)	O(2)-Co-N(7)	175.3 (1)	N(1)-Co-N(7)	89.3 (2)
N(5)-C(10)	1.322 (6)	N(6)-C(11)	1.507 (7)	N(3)-Co-N(7)	92.1 (2)	N(5)-Co-N(7)	91.5 (2)
N(6)-C(12)	1.492 (8)	C(7)-C(8)	1.365 (8)	N(6)-Co-N(7)	85.6 (2)	Co-N(1)-C(1)	129.0 (3)
C(10)-C(11)	1.506 (7)	C(12)-C(13)	1.517 (9)	C(1)-N(1)-C(3)	106.4 (5)	C(5)-N(3)-C(6)	118.2 (4)
				Co-N(6)-C(12)	107.2 (3)	Co-N(7)-C(13)	110.7 (3)
				C(3)-C(4)-C(5)	111.0 (5)	O(1)-C(6)-C(7)	120.3 (5)
				N(3)-C(6)-C(7)	111.3 (4)	N(5)-C(7)-C(6)	111.5 (5)
				N(4)-C(10)-N(5)	122.8 (4)	N(6)-C(11)-C(10)	109.5 (4)
bond distances				bond angles			
[Co(PMA)(N-MeIm)](NO ₃) ₂ ·H ₂ O (6)							
Co-N(1)	1.941 (2)	Co-N(3)	1.917 (2)	N(1)-Co-N(3)	95.6 (1)	N(1)-Co-N(5)	175.8 (1)
Co-N(5)	1.858 (2)	Co-N(6)	2.005 (2)	N(3)-Co-N(5)	81.5 (1)	N(1)-Co-N(6)	98.7 (1)
Co-N(7)	1.953 (4)	Co-N(8)	1.956 (3)	N(3)-Co-N(6)	165.2 (1)	N(5)-Co-N(6)	84.0 (1)
O(1)-C(6)	1.239 (3)	N(1)-C(1)	1.331 (3)	N(1)-Co-N(7)	88.3 (1)	N(3)-Co-N(7)	91.2 (1)
N(1)-C(3)	1.392 (3)	N(3)-C(5)	1.465 (3)	N(5)-Co-N(7)	88.8 (1)	N(6)-Co-N(7)	85.7 (1)
N(3)-C(6)	1.334 (3)	N(4)-C(10)	1.331 (3)	N(1)-Co-N(8)	91.2 (1)	N(3)-Co-N(8)	90.1 (1)
N(6)-C(11)	1.495 (3)	N(6)-C(12)	1.502 (5)	N(5)-Co-N(8)	91.8 (1)	N(6)-Co-N(8)	93.2 (1)
N(8)-C(14)	1.331 (4)	N(9)-C(17)	1.459 (4)	N(7)-Co-N(8)	178.6 (1)	H(8A)-O(8)-H(8B)	108 (4)
C(7)-C(8)	1.378 (3)	C(10)-C(11)	1.496 (4)	Co-N(1)-C(1)	130.3 (2)	C(1)-N(1)-C(3)	106.1 (2)
C(12)-C(13)	1.503 (4)	C(15)-C(16)	1.348 (5)	C(5)-N(3)-C(6)	118.3 (2)	Co-N(6)-C(12)	106.8 (2)
				Co-N(7)-C(13)	110.4 (2)	C(3)-C(4)-C(5)	113.7 (3)
				O(1)-C(6)-C(7)	121.4 (2)	N(3)-C(6)-C(7)	110.3 (2)
				N(4)-C(10)-N(5)	122.9 (2)	N(6)-C(11)-C(10)	110.0 (2)
				N(8)-C(14)-N(9)	110.8 (3)	N(9)-C(15)-C(16)	106.5 (3)
bond distances				bond angles			
[Co(PMA)Cl]Cl·EtOH (7)							
Co-Cl(1)	2.258 (2)	Co-N(1)	1.923 (5)	Cl(1)-Co-N(1)	89.8 (2)	Cl(1)-Co-N(3)	91.8 (2)
Co-N(3)	1.910 (5)	Co-N(5)	1.851 (5)	N(1)-Co-N(3)	95.9 (2)	Cl(1)-Co-N(5)	88.7 (2)
Co-N(6)	1.996 (5)	Co-N(7)	1.956 (5)	N(1)-Co-N(5)	177.6 (2)	N(3)-Co-N(5)	82.3 (2)
O(1)-C(6)	1.240 (7)	N(1)-C(1)	1.326 (9)	Cl(1)-Co-N(6)	92.0 (1)	N(1)-Co-N(6)	97.6 (2)
N(1)-C(3)	1.396 (8)	N(3)-C(5)	1.455 (8)	N(3)-Co-N(6)	166.0 (2)	N(5)-Co-N(6)	84.3 (2)
N(3)-C(6)	1.337 (8)	N(4)-C(10)	1.340 (8)	Cl(1)-Co-N(7)	177.5 (1)	N(1)-Co-N(7)	91.3 (2)
N(5)-C(10)	1.336 (7)	N(6)-C(11)	1.490 (8)	N(3)-Co-N(7)	90.4 (2)	N(5)-Co-N(7)	90.3 (2)
N(6)-C(12)	1.493 (8)	C(7)-C(8)	1.372 (9)	N(6)-Co-N(7)	85.6 (2)	Co-N(1)-C(1)	128.1 (4)
C(10)-C(11)	1.494 (8)	C(12)-C(13)	1.505 (8)	C(1)-N(1)-C(3)	106.6 (5)	C(5)-N(3)-C(6)	118.4 (5)
				Co-N(6)-C(12)	107.6 (3)	Co-N(7)-C(13)	110.1 (3)
				C(3)-C(4)-C(5)	113.6 (5)	O(1)-C(6)-C(7)	120.8 (5)
				N(3)-C(6)-C(7)	110.7 (5)	N(5)-C(7)-C(6)	111.0 (5)
				N(4)-C(10)-N(5)	123.0 (5)	N(6)-C(11)-C(10)	110.7 (5)

oxygens of the nitrate ions and the coordinated amine groups as well as the imidazole N-H moiety (viz. N(6)-O(5) = 2.939 (3) Å, N(2)-O(2) = 2.800 (3) Å). The cobalt atom is octahedrally coordinated by six N atoms, five from the deprotonated PMA⁻ ligand and one from the N-MeIm molecule. As expected, the various Co(III)-N distances in **6** are very similar to those in **5** (the Co(III)-N(1) and Co(III)-N(7) are both slightly longer in **6**, Table II). Also, the two Co(III)-N_{im} distances, namely, Co(III)-N(1) and Co(III)-N(8) are quite close to each other.

In **6**, the dihedral angle between plane 1 and the imidazole ring is smaller (13.6°) compared to that in **5** (Figure 2). The N-MeIm ring is almost perpendicular to the mean basal plane and is positioned such that the methyl group (C(17)) is away from the carbonyl oxygen (O(1)).

Structure of [Co(PMA)Cl]Cl·EtOH (7). The structure of the cation is represented in Figure 3, while selected bond distances and angles are collected in Table II. The Co(III) center is octahedrally coordinated by five nitrogens from the PMA⁻ ligand and a chloride ion. Metric parameters of the coordinated PMA⁻ framework in this complex as well as the Co(III)-N distances are quite comparable to those observed in **5** and **6** (Table II). The Co(III)-Cl distance (2.258 (2) Å) compares well with the same reported for other cobalt(III) complexes.^{53,56} A dihedral angle

of 18.6° is noted between plane 1 and the plane of the imidazole ring of PMA⁻ ligand in **7**. H-bonding interaction is evident between the ligand chloride and the imidazole NH of the neighboring cation as well as between the oxygen atom of lattice ethanol and the secondary amine group (N(6)) of the PMA⁻ ligand.

Properties. Electronic Absorption Spectra. The present complexes **5-7** are derived from the designed ligand PMAH which closely resembles the metal-binding locus of BLM. Therefore, color match between these complexes and the corresponding Co(III)-BLMs deserve special attention. Listed in Table III are the absorption maxima (λ_{max} , nm) and the extinction coefficients (ϵ , M⁻¹ cm⁻¹) of the band in the visible region for the cobalt(III) complexes of PMAH, BLM, and pseudotetrapeptide A. Even though no ϵ values are reported for the Co(III)-BLMs,²⁰ it is quite apparent from Table III that the present complexes **5-7** do exhibit colors similar to the corresponding Co(III)-BLMs. In water, the λ_{max} of **7** is somewhat blue-shifted compared to GREEN Co-

(56) (a) Zimmer-Gasser, B.; Dash, K. C. *Inorg. Chim. Acta* **1980**, *55*, 43. (b) Matsumoto, K.; Ooi, S.; Kuroya, H. *Bull. Chem. Soc. Jpn.* **1970**, *43*, 380. (c) Messmer, G. G.; Amma, E. L. *Acta Crystallogr.* **1968**, *B24*, 417. (d) Ooi, S.; Kuroya, H. *Bull. Chem. Soc. Jpn.* **1963**, *36*, 1083.

Table III. Absorption Spectral Data

complex	color	λ_{\max} , nm (ϵ , $M^{-1} \text{cm}^{-1}$)	
		water	DMSO
[Co(PMA)(H ₂ O)](NO ₃) ₂ (5)	brown	540 (90)	555 (108) ^a
[Co(PMA)(N-MeIm)](NO ₃) ₂ ·H ₂ O (6)	orange	520 (120)	520 (155)
[Co(PMA)Cl]Cl·EtOH (7)	green	580 (108)	590 (140)
aquo-Co(III)-BLM	BROWN	544 ^b	
Co(III)-BLM	ORANGE	520 ^b	
HOO-Co(III)-BLM	GREEN	594 ^b	
Co(III)-pseudotetrapeptide A	red brown	550 (136) ^c	

^aSpectrum recorded is that of [Co(PMA)(DMSO)]²⁺. ^bRef 20. ^cRef 21.

(III)-BLM. However, as discussed earlier, 7 is converted into 5 in aqueous solution, and this fact does not allow one to measure the λ_{\max} value accurately. In DMSO, 7 does not convert into 5 and in this solvent 7 exhibits its λ_{\max} at 590 nm, a value very close to the λ_{\max} of GREEN Co(III)-BLM in water (594 nm).

Dabrowiak et al. have assigned the electronic absorption spectrum of the cobalt(III) complex of pseudotetrapeptide A.²¹ This complex exhibits a band at 550 nm which has been assigned to the ¹A₁ → ¹E transition of the low-spin d⁶ Co(III) center. With 5-7, the absorption band in the visible region presumably arises from the same transition. This is supported by the blue-shift of the band as the sixth ligand changes from Cl⁻ to H₂O to N-MeIm in 7-5 (Table III). That the sixth ligand on cobalt in the pseudotetrapeptide complex is H₂O is also supported by the data in Table III. Since PMAH lacks quite a few chromophores which are present in BLM, comparison of the high energy side of the electronic spectra of the present complexes with those of Co(III)-BLMs is not feasible. Nevertheless, data in Table III indicate that the architectures of the coordination spheres around cobalt in 5-7 approach those in Co(III)-BLMs quite closely. The only difference is GREEN Co(III)-BLM in which the sixth ligand is believed to be a -OOH group instead of Cl⁻ in 7.⁵⁷ However, similarities in reactivity of 7 and GREEN Co(III)-BLM, discussed in the forthcoming sections, allows 7 to qualify as a good model of GREEN Co(III)-BLM.

NMR Spectra. The ¹H and ¹³C NMR spectra of 5-7 have been run in (CD₃)₂SO, and the chemical shifts for the various peaks are listed in Table IV. Both ¹H-¹H and ¹H-¹³C COSY results as well as APT and DEPT data have been used to assign all the resonances. As representative examples, the ¹H and ¹³C spectra of [Co(PMA)(DMSO)](NO₃)₂·H₂O (the H₂O ligand of the complex 5 is replaced by DMSO on standing in solution, vide infra) are shown in Figure 4, while the ¹H-¹³C COSY spectrum is displayed in Figure 5. In both figures as well as in Table IV, resonances corresponding to the various hydrogen and carbon atoms of the complexes have been labeled in accordance with the X-ray structures (Figures 1-3).

The chemical shifts of the nonexchangeable imidazole protons H1 and H2 of coordinated PMA⁻ ligand are quite sensitive to the sixth ligand on cobalt (Table IV). For example, with freshly prepared solution of 5 in (CD₃)₂SO (when H₂O is still the sixth ligand), H1 and H2 resonate at 8.75 and 7.55 ppm, respectively. On standing, H₂O is replaced by (CD₃)₂SO, and the two peaks move to 8.81 and 7.59 ppm (Figure 4). The same behavior has also been reported by Dabrowiak et al. in the NMR spectra of the cobalt(III) complex of pseudotetrapeptide A²¹ and this in turn reconfirms that the sixth ligand on cobalt in the pseudotetrapeptide A complex is indeed H₂O. The kinetics of the displacement of H₂O by DMSO have been studied in the present study (vide infra).

(57) The qualitative "ferricyanide test" used by Chang et al.²⁰ in identifying the -OOH group in GREEN Co(III)-BLM requires one comment. We have performed this test with 7 as well as a number of cobalt(III) complexes. Positive result (blue precipitate) is obtained not only with 7 and 5 (6 is not responsive) but also with complexes like [Co(His)₂]ClO₄ (His = histidinato ligand) and [Co(acac)₃] (acac = acetylacetonato ligand). Complexes like *trans*-[Co(py)₂Cl₂]Cl and simple cobalt(II) salts do not yield blue precipitate, while [Co(NH₃)₅Cl]²⁺ affords blue precipitate slowly over 2-3 h. This test for -OOH group is clearly not conclusive.

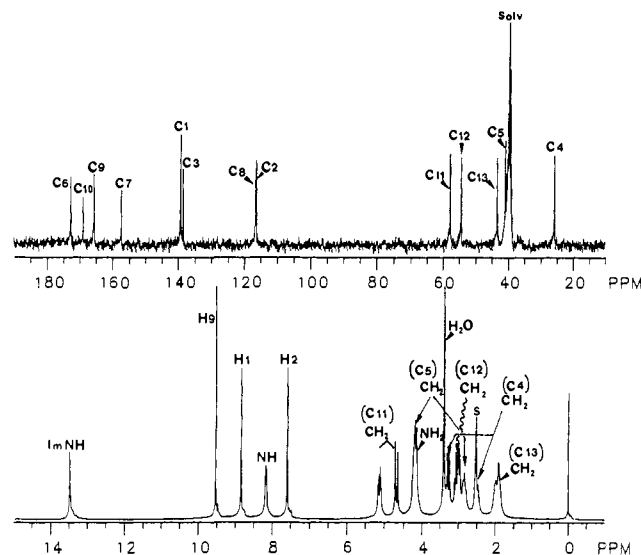


Figure 4. ¹H (lower trace) and ¹³C (upper trace) NMR spectra (300 MHz, 293 K) of [Co(PMA)((CD₃)₂SO)](NO₃)₂·H₂O (see text) in (CD₃)₂SO. Signal assignments (see Figure 1) are indicated.

Interestingly, another resonance which is susceptible to the sixth ligand on cobalt in the single H (H9) on the pyrimidine ring of PMA⁻ (Table IV). The imidazole NH peak of the coordinated PMA⁻ ligand appears at relatively low field (~13 ppm) presumably due to donation of electron density by N1 to cobalt. This is discussed in detail in refs 40 and 50. Assignment of the NH and NH₂ peaks (both disappear in D₂O, Table IV, also see supplementary material) is supported by their positions in the NMR spectrum of the [Co(dien)₂]³⁺ (dien = diethylenetriamine) complex in (CD₃)₂SO⁵⁸ and the intensity ratio.⁵⁹

The ¹H NMR spectra of 5-7 contain an interesting doublet-doublet-triplet-triplet (ddtt) pattern for the four hydrogens of the two CH₂ groups (C4 and C5) that bridge the peptide nitrogen and the imidazole ring of the coordinated PMA⁻ ligand (Figure 4). The ¹H-¹³C COSY spectra (Figure 5 is an example) indicate that this pattern arises from the four mutually coupled hydrogen atoms (¹H-¹³C COSY) resonating at four distinctly different positions (Table IV). The ddtt pattern is more clearly discernable in the NMR spectra in D₂O solutions (Figure 6). A somewhat different (dtdt) pattern for these four hydrogens was first observed in the NMR spectra of 9 and related complexes.^{40,50} For more discussion and the values of the various coupling constants, refs 40 and 50 are recommended. The two CH₂ groups (C12, C13) between the NH and NH₂ functions give rise to peaks around 3 and 2 ppm (Table IV), while the single CH₂ (C11) between the NH group and the pyrimidine ring exhibits a complicated AB pattern around 4.5-5.0 ppm. In D₂O solutions, the latter CH₂ group, however, gives rise to a clean AB pattern (compare Figures 4 and 6). The simplification of the AB pattern demonstrates coupling between the NH and the two hydrogens on C11. The NH-CH₂ (C11) and NH₂-CH₂ (C13) connectivities are also revealed in the ¹H-¹H COSY spectra.

Resonances for the solvent molecules of crystallization in the present complexes have been properly identified (Table IV). The N-MeIm ligand in 6 gives rise to peaks at 6.16, 7.19, and 7.24 for ring protons, while the CH₂ group resonates at 3.56 ppm.

Thirteen distinct resonances for the 13 carbon atoms of the PMA⁻ ligand have been located in the ¹³C NMR spectra of all three complexes (Table IV). A significant number of peaks in these spectra have been identified with the aid of the completely assigned NMR spectrum of 9⁵⁰ and APT data.⁶⁰ Downfield shift

(58) Yoshikawa, Y.; Yamasaki, K. *Bull. Chem. Soc. Jpn.* 1972, 45, 179.

(59) In the cobalt(III) complex of pseudotetrapeptide A, the NH and NH₂ group of the β-aminoalanine portion resonate at 7.94 and 4.30 ppm, respectively (solv = (CD₃)₂SO).²¹

(60) APT results clearly point out the resonances for the quaternary carbon atoms (C3, C6, C7, C8, and C10) and the CH₂ groups.

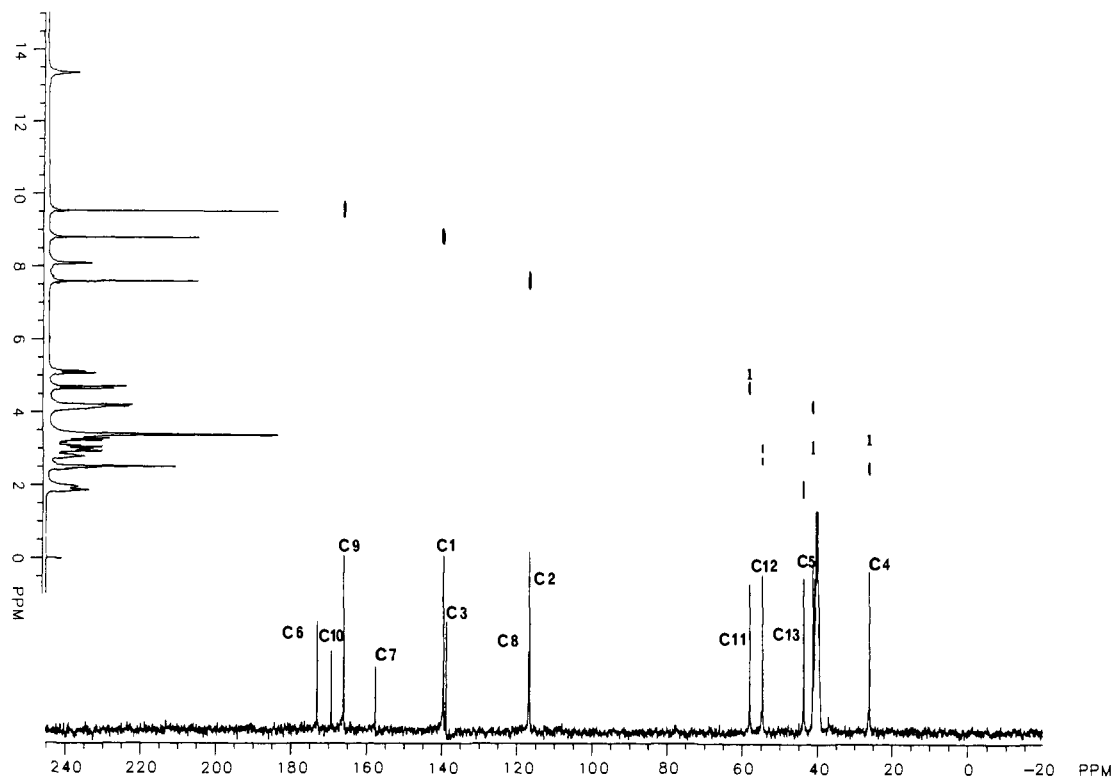


Figure 5. ^1H - ^{13}C ($J = 140$ Hz) COSY spectrum of $[\text{Co}(\text{PMA})((\text{CD}_3)_2\text{SO})](\text{NO}_3)_2 \cdot \text{H}_2\text{O}$ in $(\text{CD}_3)_2\text{SO}$.

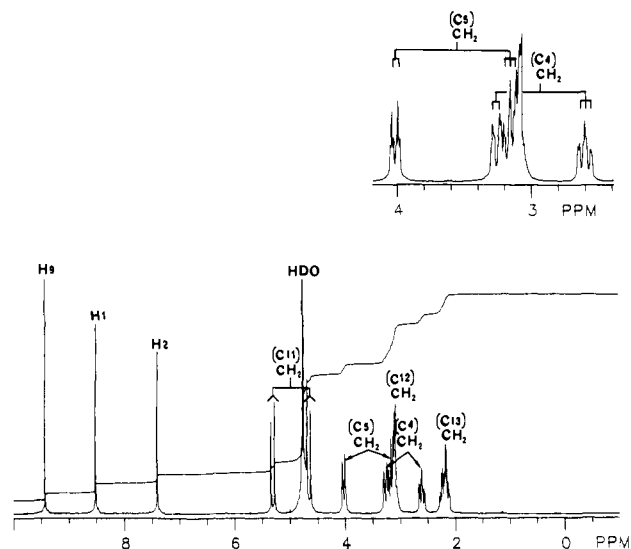


Figure 6. ^1H NMR spectrum (300 MHz, 293 K) of **5** in D_2O . Inset: the 2.5–4.0 ppm region, expanded.

of the carbonyl (C6) peak (from 167.28 ppm in PMAH²³ to 172–173 ppm in **5–7**) is observed in each case as a result of coordination of the peptide nitrogen (N3) to cobalt. Similar shift has been noted with **9**⁴⁰ and other peptide complexes.^{50,61} The C1 resonance also moves downfield (from 134.53 ppm in PMAH²³ to ~ 139 ppm) due to coordination of the imidazole nitrogen N1 to the metal center in **5–7**. Assignments of the C1, C2, C4, C5, C9, C11, C12, and C13 peaks rely on the ^1H - ^{13}C COSY results (Figure 5, for example), while resonances due to the pyrimidine ring carbons have been identified by comparing the ^{13}C NMR spectra of **5–7**, with **2**, **9**, and related complexes.

The kinetics of the two reactions $\mathbf{5} \rightarrow [\text{Co}(\text{PMA})(\text{DMSO})]^{2+}$ and $\mathbf{7} \rightarrow [\text{Co}(\text{PMA})(\text{D}_2\text{O})]^{2+}$ have been studied by NMR tech-

niques. Close inspection of the earlier ^1H NMR spectrum of **5** in $(\text{CD}_3)_2\text{SO}$ revealed that with time, the growth of one set of peaks in the 7–10 ppm region was coupled with the decline of another. It quickly became apparent that the NMR solvent $(\text{CD}_3)_2\text{SO}$ replaces the water molecule from the coordination sphere of cobalt in **5**. In analogous reaction, replacement of H_2O by DMSO in $[\text{Co}(\text{NH}_3)_5(\text{H}_2\text{O})]^{3+}$ is reported.⁶² With the $\mathbf{5} \rightarrow [\text{Co}(\text{PMA})(\text{DMSO})]^{2+}$ reaction, small downfield shifts of the peaks in the 7–10 ppm region are observed for the product as compared to the starting complex **5**. Figure 7 includes the results of the NMR experiment which clearly demonstrates the ligand exchange (H_2O by DMSO) reaction.⁶³ The inset in Figure 7 contains a kinetic plot of the decrease in the relative height (h_i/h_o) of the pyrimidine ring proton H9 of $[\text{Co}(\text{PMA})(\text{H}_2\text{O})](\text{ClO}_4)_2$. The linear behavior of the plot of $\ln(h_i/h_o)$ vs time indicates the pseudo-first-order reaction kinetics of the ligand substitution reaction with $k = 2.1 \times 10^{-2} \text{ min}^{-1}$ (313 K).⁶⁴ A similar experiment afforded $k = 4.18 \times 10^{-3} \text{ min}^{-1}$ (293 K) for the reaction $\mathbf{7} \rightarrow [\text{Co}(\text{PMA})(\text{D}_2\text{O})]^{2+}$. These results clearly suggest that ligand exchange is a quite facile and feasible reaction at the cobalt center in BROWN and GREEN Co(III)-BLMs for which H_2O and $-\text{OOH}$ have been respectively proposed as the sixth ligand.⁶⁵

DNA Cleavage Reactions. Like GREEN and BROWN Co(III)-BLMs, the analogue complexes **5–7** induce strand breaks in DNA under UV illumination. For example, irradiation of supercoiled covalently closed circular ϕX174 DNA in the presence of submillimolar amount of **5** results in progressive appearance of nicked circular (form II) and linear duplex (form III) DNA in lanes 4, 6, 8, and 10 of Figure 8A. No strand scission is observed in the dark (lane 2, Figure 8A), while the UV light alone causes

(62) Buckingham, D. A.; Marty, W.; Sargeson, A. M. *Inorg. Chem.* 1974, 13, 2165.

(63) A 20-mg sample of $[\text{Co}(\text{PMA})(\text{H}_2\text{O})](\text{ClO}_4)_2$ was quickly dissolved in 0.6 mL of $(\text{CD}_3)_2\text{SO}$. The substitution reaction at 313 K was followed by recording a new ^1H NMR spectrum every 6.7 min for 2 h. For each spectrum, 40 free induction decays (FIDs) were accumulated. The time from mixing to the 20th FID was taken as the time for each spectrum (Figure 7).

(64) The same value of k was obtained from plots of $\ln(h_i/h_o)$ vs time for the H1 and H2 peaks (Figure 7).

(65) Chang et al. have reported ligand replacement reactions with BROWN Co(III)-BLM.²⁰

(61) (a) Hawkins, C. J.; Martin, J. *Inorg. Chem.* 1986, 25, 2146. (b) Boas, L. V.; Evans, C. A.; Gillard, R. D.; Mitchell, P. R.; Phipps, D. A. *J. Chem. Soc., Dalton Trans.* 1979, 582.

Table IV. NMR Data (300 MHz, (CD₃)₂SO, 293 K, δ from TMS)

	[Co(PMA)(H ₂ O)](NO ₃) ₂ (5) ^{a,b}	Co(PMA)(DMSO)](NO ₃) ₂ ^c	[Co(PMA)(N-MeIm)](NO ₃) ₂ H ₂ O (6)	[Co(PMA)Cl]Cl-EtOH (7)
¹ H NMR				
H1	8.75 (1 H, s, im)	8.81 (1 H, s, im)	8.51 (1 H, s, im)	8.95 (1 H, s, im)
H2	7.55 (1 H, s, im)	7.59 (1 H, s, im)	7.47 (1 H, s, im)	7.35 (1 H, s, im)
H4	2.51 (1 H, t, J = 12 Hz)	2.51 (1 H, t, J = 12 Hz)	2.63 (1 H, t, J = 12 Hz)	2.53 (1 H, t, J = 12 Hz)
	3.18 (1 H, d, J = 14 Hz)	3.26 (1 H, d, J = 14 Hz)	2.99 (1 H, d, J = 14 Hz)	3.09 (1 H, d, J = 14 Hz)
H5	2.81 (1 H, t, J = 12 Hz)	2.79 (1 H, t, J = 12 Hz)	2.83 (1 H, t, J = 12 Hz)	2.78 (1 H, t, J = 12 Hz)
	3.99 (1 H, d, J = 14 Hz)	4.10 (1 H, d, J = 14 Hz)	3.76 (1 H, d, J = 14 Hz)	3.93 (1 H, d, J = 14 Hz)
H9	9.51 (1 H, s, H9 of pm)	9.54 (1 H, s, H9 of pm)	9.49 (1 H, s, H9 of pm)	9.36 (1 H, s, H9 of pm)
H11	4.69, 5.10 (2 H, ABq, J _{AB} = 19 Hz)	4.67, 5.10 (2 H, ABq, J _{AB} = 19 Hz)	4.58, 5.05 (2 H, ABq, J _{AB} = 19 Hz)	4.56, 4.96 (2 H, ABq, J _{AB} = 19 Hz)
H12	2.97 (2 H, m)	3.01 (2 H, m)	3.00 (2 H, m)	2.89 (2 H, m)
H13	1.89 (2 H, m)	1.87 (2 H, m)	2.17 (2 H, m)	1.97 (2 H, m)
HN2	13.31 (1 H, s, NH of im)	13.37 (1 H, s, NH of im)	13.28 (1 H, s, NH of im)	13.76 (1 H, s, NH of im)
HN6	7.97 (1 H, s, NH)	8.10 (1 H, s, NH)	7.92 (1 H, s, NH)	8.31 (1 H, s, NH)
H ₂ N7	4.17 (2 H, NH ₂)	4.17 (2 H, NH ₂)	4.62 (2 H, NH ₂)	4.24 (2 H, NH ₂)
	3.39 (2 H, s, H ₂ O)	3.38 (2 H, s, H ₂ O)	7.19 (1 H, s, C14 of N-MeIm)	1.05 (CH ₃ of EtOH)
			6.16 (1 H, s, C15 of N-MeIm)	3.44 (CH ₂ of EtOH)
			7.24 (1 H, s, C16 of N-MeIm)	
			3.56 (3 H, s, C17 of N-MeIm)	
			3.32 (2 H, s, H ₂ O)	
¹³ C NMR				
C1	138.60	139.45	139.60	139.74
C2	115.60	116.56	116.53	114.25
C3	137.93	138.76	138.25	137.93
C4	25.23	26.11	26.25	25.95
C5	40.27	41.22	40.61	40.31
C6	172.08	173.05	171.74	171.94
C7	156.84	157.60	157.58	157.99
C8	115.87	116.86	117.84	115.60
C9	164.93	165.96	165.77	163.49
C10	168.29	169.29	167.96	167.49
C11	57.27	57.99	58.00	57.55
C12	53.72	54.60	55.90	55.26
C13	42.94	43.67	42.59	41.52
C14			124.12	
C15			127.43	
C16			139.72	
C17			35.20	

^aSpectrum was run with a freshly prepared solution (within 2 min). ^bIn D₂O (pD = 5.8), [Co(PMA)(H₂O)](ClO₄)₂ gives rise to the following peaks (read the table in the same order): H1, 8.52 (1 H, s, im); H2, 7.39 (1 H, s, im); H4, 2.60 (1 H, t, J = 14 Hz); 3.26 (1 H, d, J = 16.0 Hz); H5, 3.16 (1 H, t, J = 14 Hz); 4.02 (1 H, d, J = 14 Hz); H9, 9.43 (1 H, s, H9 of pm); H11, 4.64, 5.30 (2 H, ABq, J_{AB} = 19 Hz); H12, 3.08 (2 H, m); H13, 2.20 (2 H, m); HOD, 4.75; C1, 138.54; C2, 116.62; C3, 137.94; C4, 25.57; C5, 41.21; C6, 171.59; C7, 158.07; C8, 117.72; C9, 167.00; C10, 169.64; C11, 58.64; C12, 54.84; C13, 43.05. ^cThe H₂O ligand of 5 is replaced by DMSO on standing in (CD₃)₂SO solution. The limiting spectrum is reported herein.

only small damage to DNA (lanes 3, 5, 7 and 9). When compared to the respective Co(III)-BLMs, the extent of DNA damage by the PMAH complexes 5 and 7 is somewhat diminished (Figure 8B). This is however expected since 5 and 7 do not possess any group like the bithiazole group or the positively-charged amine tail of BLM that assists the Co(III)-BLMs to bind tightly to the DNA helix. DNA damage by 5-7 is still possible due to electrostatic binding of the complex cations to the negatively-charged phosphate backbone of DNA as well as the finite probability of bimolecular collisions. Electrostatic binding to DNA by 5-7 has been confirmed by monitoring the extent of strand scission with increasing amount of Na₂SO₄ in the incubation mixture. As shown in Figure 9A, increasing concentration of Na₂SO₄ in mixtures of form I Φ X174 DNA and 5 results in a steady diminution of form II DNA produced during 1 h of UV illumination. With 50 mM Na₂SO₄, complete protection of DNA is noted (lane 7, Figure 9A).

In earlier accounts, it has been suggested that the cleavage of DNA could be a consequence of photoreduction of Co(III)-BLMs.¹⁵ Indeed, many cobalt(III) complexes are known to release the labile Co²⁺ ions upon UV irradiation.⁶⁶ Since Co²⁺ ions cause

DNA damage,⁶⁷ one has to be cautious about the release of Co²⁺ ions from 5-7 in solution upon illumination. Though with polycyclic ligands like PMAH (and BLM), release of Co²⁺ ions as a result of photoreduction of the cobalt(III) species is quite unlikely (Co²⁺ will not readily escape the coordination sphere), we have looked into this possibility. No change in the electronic absorption spectra has been noted with photolyzed solutions of 5-7 in buffer solutions that are used in the DNA cleavage experiments.⁶⁸ Also, no trace of Co²⁺ has been detected in such solutions by the analytical method using KSCN. In addition, significant DNA strand scission is only monitored in the presence of very high concentration of Co²⁺ ions under our experimental conditions (Figure 9B). Clearly, photoinduced DNA damage by 5-7 (and presumably Co(III)-BLMs) is not a consequence of photoreduction.

Characteristics of the light-induced DNA cleavage reaction by 5-7 are strikingly similar to those reported for Co(III)-BLMs. Much like the decreasing order of DNA damage capacity of the

(67) (a) Jensen, A. A.; Tuchsén, F. *Crit. Rev. Toxicol.* **1990**, *20*, 427. (b) Matzcu, M.; Mazzei, F.; Minoprio, A. *Studia Biophys.* **1989**, *131*, 177.

(68) The complexes 5-7 were photolyzed at different wavelengths (both in the d-d and charge-transfer regions) in these attempts. A Carl Zeiss UV generator with various filters was used for photolysis.

(66) See, for example: Adamson, A. W. *Coord. Chem. Rev.* **1968**, *3*, 169.

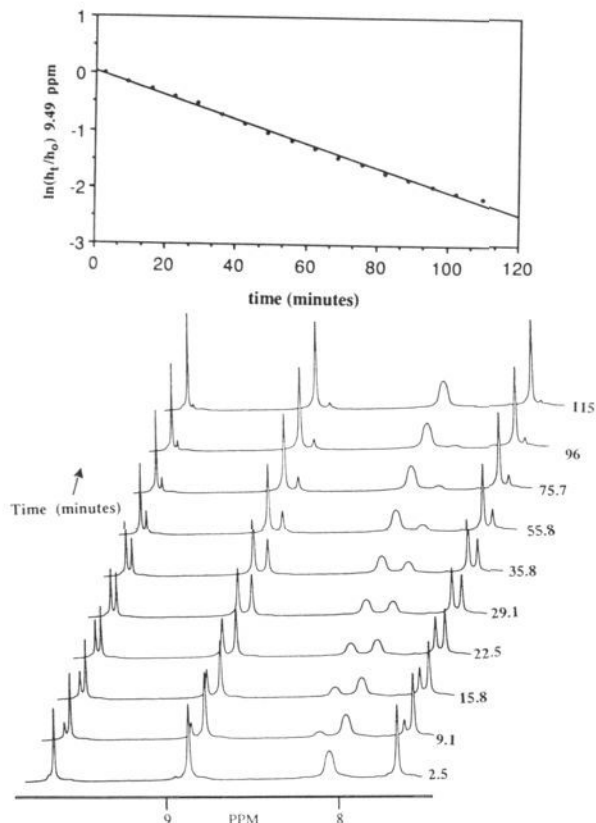


Figure 7. Time-dependent changes in the 7.5–10-ppm region of the ^1H NMR spectrum of **5** in $(\text{CD}_3)_2\text{SO}$ as a result of the ligand-displacement reaction $[\text{Co}(\text{PMA})(\text{H}_2\text{O})]^{2+} \rightarrow [\text{Co}(\text{PMA})(\text{CD}_3)_2\text{SO}]^{2+}$ at 313 K (see text for detail). Inset: plot of the relative height ($\ln(h_1/h_0)$) of the pyrimidine proton H9 vs. time.

$\text{Co}(\text{III})$ -BLMs GREEN > BROWN > ORANGE,¹⁶ the extent of DNA nicking by the present complexes follows the order $7 > 5 > 6$. Also, the DNA cleavage reaction by **5–7** is insensitive to the presence of dioxygen in the reaction mixture. In fact, when irradiated in a N_2 -filled glove bag, submillimolar concentrations of **5–7** in rigorously degassed buffer inflicted more damage to form I $\text{OX}174$ DNA compared to that observed in regular experiments under aerobic conditions. Similar results have been reported for $\text{Co}(\text{III})$ -BLMs.¹⁶ In addition, like $\text{Co}(\text{III})$ -BLMs, DNA cleavage reactions with **5–7** do not generate base propenals.^{69,70} This is to be expected since formation of base propenals in the DNA degradation reactions by M-BLMs requires dioxygen (viz. in DNA cleavage reaction by Fe-BLM).³ Collectively, the latter two facts rule out the oxidative pathway of DNA damage in case of $\text{Co}(\text{III})$ -BLMs and the analogues **5–7**. Saito et al.^{13a} have recently proposed that BROWN $\text{Co}(\text{III})$ -BLM degrades DNA only after it is converted into GREEN $\text{Co}(\text{III})$ -BLM through photoreduction of $\text{Co}(\text{III})$ to $\text{Co}(\text{II})$ and reoxidation by O_2 (when $-\text{OOH}$ group appears as the sixth ligand on cobalt). Experiments in this laboratory as well as the report by Meares and co-workers¹⁶ contradict this suggestion. BROWN $\text{Co}(\text{III})$ -BLM does cleave DNA in the absence of dioxygen. Results discussed in the next section, on the other hand, point out to a mechanism of DNA degradation by **5–7** and $\text{Co}(\text{III})$ -BLMs that does not require dioxygen at all.⁷¹

(69) Reaction mixtures containing 25 mM Tris-borate buffer (pH 8) and 1 mg/mL calf thymus DNA were irradiated with 5 mM **5** for 3 h at 320 nm. Aliquots (0.5 mL) were then mixed with 0.5 mL of thiobarbituric acid (1% in 0.05 M NaOH) and 0.5 mL of trichloroacetic acid (28%), and the mixtures were heated to 95 °C for 20 min. Detection of the colored product was performed at 532 nm.⁷⁰

(70) (a) Quinlan, G. J.; Gutteridge, J. M. C. *Biochem. Pharmacol.* **1987**, *36*, 3629. (b) Giloni, L.; Takeshita, M.; Johnson, F.; Iden, C.; Grollman, A. P. *J. Biol. Chem.* **1981**, *256*, 8608.

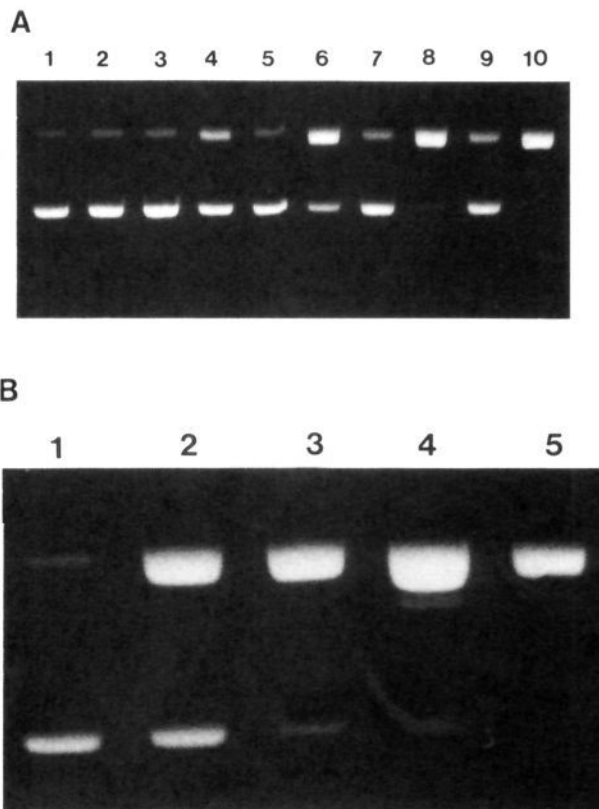


Figure 8. (A) $\text{OX}174$ (RF) DNA cleavage experiment with $[\text{Co}(\text{PMA})(\text{H}_2\text{O})](\text{NO}_3)_2$ (**5**) in 25 mM Tris-borate, 190 μM EDTA, pH 8.1 buffer at 298 K. Each reaction mixture contained 1 μg of DNA in a total volume of 40 μL . Concentration of **5** used = 5×10^{-4} M: lane 1, DNA, dark, 3 h; lane 2, DNA + **5**, dark, 3 h; lane 3, DNA, UV light, 15 min; lane 4, DNA + **5**, UV light, 15 min; lane 5, DNA, UV light, 1 h; lane 6, DNA + **5**, UV light, 1 h; lane 7, DNA, UV light, 2 h; lane 8, DNA + **5**, UV light, 2 h; lane 9, DNA, UV light, 3 h; lane 10, DNA + **5**, UV light 3 h. (B) DNA cleavage experiment with **5**, **7**, and BROWN and GREEN $\text{Co}(\text{III})$ -BLMs in the above-mentioned buffer solution. DNA (1.6 μg) in a total volume of 40 μL buffer was used. Irradiation was done at 320 nm for 2 h: lane 1, DNA; lane 2, DNA + $\sim 5 \mu\text{M}$ BROWN $\text{Co}(\text{III})$ -BLM; lane 3, DNA + $\sim 5 \mu\text{M}$ GREEN $\text{Co}(\text{III})$ -BLM; lane 4, DNA + 0.5 mM **5**; lane 5, DNA + 0.5 mM **7**.

Spin-Trapping Experiments. In the presence of DMPO as the spin trap, irradiated solutions of **5–7** in aqueous buffer exhibit the typical four line (intensity ratio 1:2:2:1, $A_N = A_H = 15$ G) ESR spectrum of $\cdot\text{OH}$ radical⁷³ (Figure 10). Interestingly, the green complex **7** affords a higher concentration of the spin adduct (as judged by spin integration, middle trace of Figure 10) compared to **5** and **6**. It is clear from Figure 10 that $\cdot\text{OH}$ radicals are formed rather quickly (within min) with 1 mM solutions of **5–7**. With concentrations in the μM range, ESR signals of appreciable intensities are recorded within 30 min. It must be mentioned here that in all previously reported research,^{13,16} mixtures of DNA and $\text{Co}(\text{III})$ -BLMs were irradiated with a 150 W xenon lamp. In contrast, a 5 mW light source has been used for irradiation in the present experiments.⁷⁴ Higher concentration

(71) $\text{Co}(\text{III})$ and other metal complexes of ligands like 1,10-phenanthroline and bipyridyl cleave DNA via the formation of singlet oxygen.⁷² The electronically excited states of the aromatic ligands sensitize molecular oxygen in such cases. Both PMAH and BLM contain pyrimidine and imidazole rings. Despite the insensitivity of the DNA cleavage reactions of **5–7** toward dioxygen in the reaction mixtures, one control experiment was performed to check the role of singlet oxygen in reactions reported here. DNA cleavage reactions were performed with **5–7** in both H_2O and D_2O media. No cleavage enhancement was noted in D_2O in any case.

(72) Fleisher, M. B.; Waterman, K. C.; Turro, N. J.; Barton, J. K. *Inorg. Chem.* **1986**, *25*, 3549.

(73) Buettner, G. R. *Free Radical Biol. Med.* **1987**, *3*, 259.

(74) Nevertheless, $\text{Co}(\text{III})$ -BLMs are overall more effective reagents for the photoinduced DNA damage compared to **5–7** (see Figure 8B).

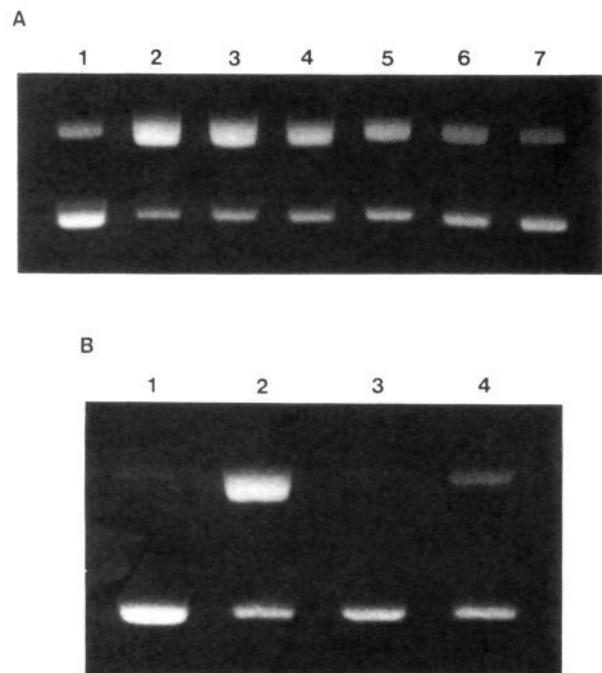


Figure 9. (A) Effect of Na_2SO_4 on the extent of DNA cleavage by $[\text{Co}(\text{PMA})(\text{H}_2\text{O})](\text{ClO}_4)_2$ in 25 mM Tris-borate, 190 μM EDTA, pH 8.1 buffer at 298 K. Each reaction mixture contained 1.6 μg of ϕX174 (RF) DNA in a total volume of 40 μL : concentration of the cobalt(III) complex = 0.5 mM; 1 h of UV illumination; lane 1, DNA; lane 2, DNA + cobalt(III) complex + 1 mM Na^+ ; lane 3, DNA + cobalt(III) complex + 5 mM Na^+ ; lane 4, DNA + cobalt(III) complex + 10 mM Na^+ ; lane 5, DNA + cobalt(III) complex + 20 mM Na^+ ; lane 6, DNA + cobalt(III) complex + 50 mM Na^+ ; lane 7, DNA + cobalt(III) complex + 100 mM Na^+ . (B) DNA cleavage experiment with **5** and $\text{CoCl}_2 \cdot 6\text{H}_2\text{O}$ in the above-mentioned buffer. DNA (1.6 μg) in a total volume of 40 μL was used: 2 h of UV illumination; lane 1, DNA + 10 μM **5**, dark; lane 2, same as lane 1, light; lane 3, DNA + 1 mM $\text{CoCl}_2 \cdot 6\text{H}_2\text{O}$, dark; lane 4, same as lane 3, light.

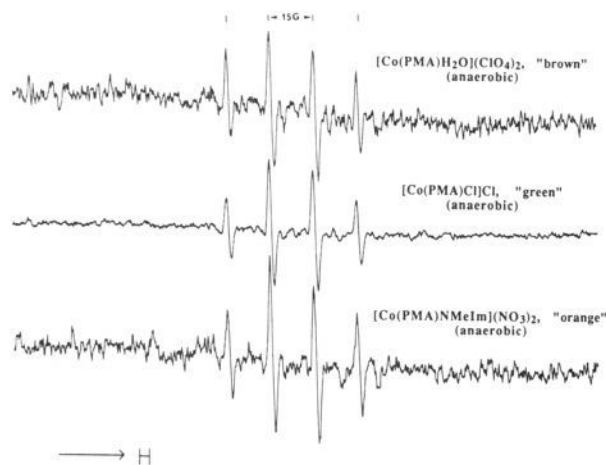


Figure 10. ESR spectra of the DMPO-OH spin adduct formed in 1 mM solution of **5** (top trace), **7** (middle trace), and **6** (bottom trace) in degassed Tris-borate buffer (pH 8) upon irradiation at 320 nm for 10 min. Concentration of the spin trap: 100 mM.

ranges have therefore been used to collect dependable spectroscopic parameters with the analogues **5-7**.

The course of $\cdot\text{OH}$ radical generation by **5-7** upon UV illumination correlates well with the extent of light-induced DNA damage by these complexes. Shown in the top panel of Figure 11 is the variation of the concentration of $\cdot\text{OH}$ radical ($[\cdot\text{OH}]$) formed in aqueous solution of **5** with time of irradiation. The values of $[\cdot\text{OH}]$ were determined by spin integration using 4-hydroxy-TEMPO (Aldrich) as the standard. Within the limi-

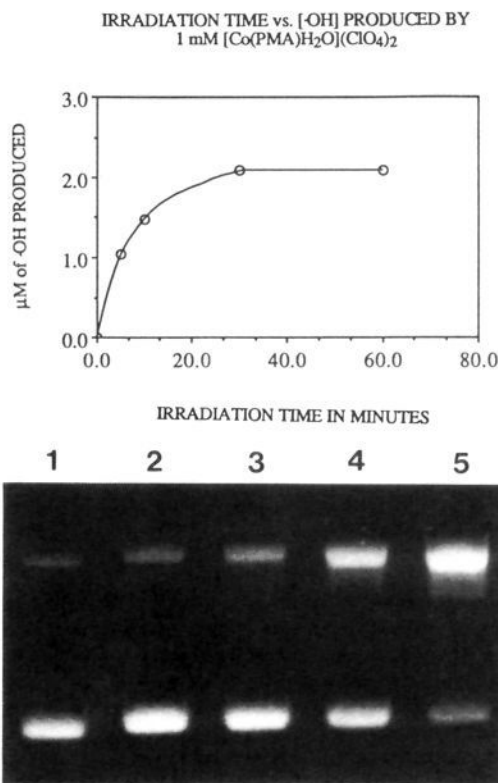


Figure 11. (Top panel) variation in $[\cdot\text{OH}]$ with irradiation time; concentration of $[\text{Co}(\text{PMA})(\text{H}_2\text{O})](\text{ClO}_4)_2$, 1 mM; concentration of spin trap, 100 mM; medium: degassed Tris-borate buffer (pH 8); wavelength of irradiation, 320 nm; (bottom panel) the extent of DNA cleavage with time (anaerobic condition) as revealed by gel electrophoresis, lane 1, ϕX174 (RF) DNA 1 $\mu\text{g}/25 \mu\text{L}$ in pH 8.1 Tris-borate buffer (25 mM) + 190 μM EDTA, 1-h irradiation at 320 nm; lane 2, same as lane 1 + 1 mM $[\text{Co}(\text{PMA})(\text{H}_2\text{O})](\text{ClO}_4)_2$, 5-min irradiation at 320 nm; lane 3, same as lane 2, 10-min irradiation at 320 nm; lane 4, same as lane 2, 30-min irradiation at 320 nm; lane 5, same as lane 2, 1-h irradiation at 320 nm.

tations of this technique,⁷⁵ it is evident that $[\cdot\text{OH}]$ reaches its maximum within 30 min. Since the $t_{1/2}$ of the decay of the DMPO-OH spin adduct is in the order of h,⁷⁶ $[\cdot\text{OH}]$ levels off shortly after this period in the absence of DNA. Parallel to this experiment was run a set of DNA cleavage reactions with **5** in which the variations in the distribution of the different forms of DNA (forms I, II, and III) in reaction mixtures with time were monitored with the aid of gel electrophoresis. The results are displayed in the bottom panel of Figure 11. It is quite apparent that more DNA strand scission is observed with longer exposure to UV light, and the extent of DNA damage follows a linear course with time at least in the first 30 min.

Results from the spin-trapping experiments with **5-7** prompted us to repeat the measurements with Co(III)-BLMs. Under similar conditions, Co(III)-BLMs produce $\cdot\text{OH}$ radical with very high efficiency. For example, as shown in Figure 12 (middle trace), $\sim 1 \mu\text{M}$ solution of GREEN Co(III)-BLM in water afforded significant concentration of the DMPO-OH spin adduct within 15 min. In fact, the Co(III)-BLMs generate $\cdot\text{OH}$ radical in such high yields that with 20–50 μM concentrations of the BLM chelates, UV illumination results in significant damage of the spin trap (since no DNA is present) and formation of a nitroxide as evidenced by a three-line ESR spectrum (intensity ratio 1:1:1, $A_N = 16 \text{ G}$,⁷⁷ bottom trace in Figure 12). That indeed the high flux of $\cdot\text{OH}$ radical generated by the Co(III)-BLM is the reason for

(75) Harbour, J. R.; Hair, M. L. *Adv. Colloid Interfac. Sci.* **1986**, *24*, 103.
 (76) Finkelstein, E.; Rosen, G. M.; Rauckman, E. J. *J. Am. Chem. Soc.* **1980**, *102*, 4994.

(77) (a) Hill, H. A. O.; Thornalley, P. J. *Inorg. Chim. Acta* **1982**, *67*, L35.
 (b) Pryor, W. A.; Govindan, C. K. *J. Am. Chem. Soc.* **1981**, *103*, 7681.

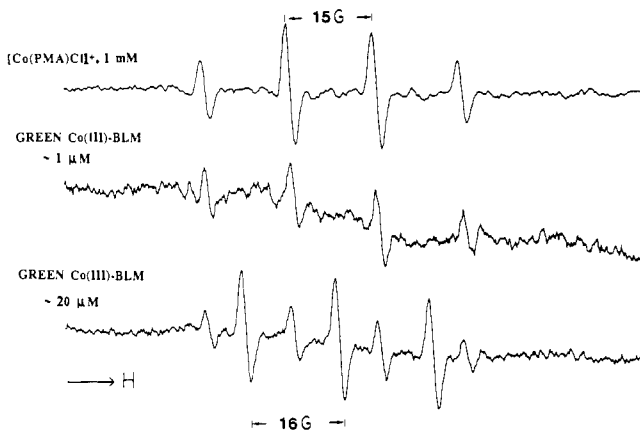


Figure 12. ESR spectra of the DMPO spin adducts under anaerobic conditions (wavelength, 320 nm; spin trap concentration, 100 mM): (top trace) complex 7, 1 mM in Tris-borate buffer (pH 8), 10-min irradiation; (middle trace) GREEN Co(III)-BLM, $\sim 1 \mu\text{M}$ in water, 15-min irradiation; (bottom trace) GREEN Co(III)-BLM, $\sim 20 \mu\text{M}$ in water, 15-min irradiation.

the spin trap damage is demonstrated by the complete absence of the nitroxide spectrum in the middle trace of Figure 12 (the same amount of spin trap was present in these two samples). It is therefore not surprising that small amounts of Co(III)-BLMs inflict extensive DNA damage upon irradiation.

Since cleavage of DNA and formation of DMPO-OH spin adduct are initiated by 5-7 (and the Co(III)-BLMs) under both aerobic and strictly anaerobic conditions, the $\cdot\text{OH}$ radical is not derived from dissolved oxygen in the buffer solutions.⁷⁸ Alternative pathways of generation of $\cdot\text{OH}$ radical were therefore looked into. In such pursuit, several reports on formation of $\cdot\text{OH}$ radical in reactions between compounds containing C/N-based radicals and water came to our attention. It is now known for quite sometime that various organic compounds including *p*-aminobenzoic acid (PABA), tryptophan, and 2-thiouracil generate $\cdot\text{OH}$ radical in aqueous solution upon UV irradiation.⁷⁹ In our hands, spin-trapping experiments with PABA and diaziquone⁸⁰ also revealed facile formation of $\cdot\text{OH}$ radical under our experimental conditions. The photoexcited products of these compounds react with water to produce $\cdot\text{OH}$ and other C/N-based radicals. We therefore performed spin-trapping experiments with 5-7 in acetonitrile under anaerobic conditions. Interestingly, complex six- to ten-line ESR spectrum of the DMPO-spin adduct (typical of C/N-based radicals) was obtained in each case (Figure 13, top trace) within 10 s of irradiation. Among several control cobalt(III) complexes, $[\text{Co}(\text{His})_2]\text{ClO}_4$ (His = histidinato) and $[\text{Co}(\text{bpy})_3](\text{ClO}_4)_3$ (bpy = bipyridine) also exhibited similar ESR spectra of spin adducts (Figure 13). These results demonstrate that in degassed nonaqueous solvents, UV irradiation leads to formation of C/N-based radical(s) when the ligands contain donor groups like pyrimidine, pyridine, imidazole, and amines. Similar spectral parameters of the top and bottom spectra in Figure 13 indicate that the imidazole ring of the coordinated PMA⁻ ligand could "house" the unpaired electron of the radical formed under UV light.

That the C/N-based radical observed with 5-7 in deaerated nonaqueous media under UV illumination rapidly generates $\cdot\text{OH}$

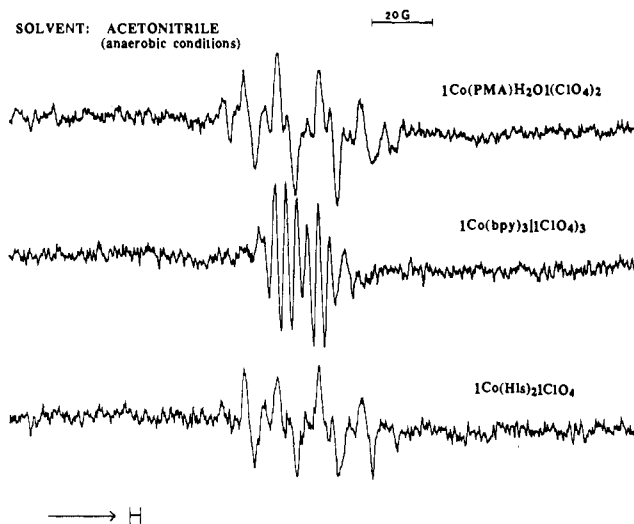


Figure 13. ESR spectra of the spin adducts of DMPO with the C/N-based radical formed in 1 mM solutions of $[\text{Co}(\text{PMA})(\text{H}_2\text{O})](\text{ClO}_4)_2$ (top trace), $[\text{Co}(\text{bpy})_3](\text{ClO}_4)_3$ (middle trace), and $[\text{Co}(\text{His})_2]\text{ClO}_4$ (bottom trace) in deaerated acetonitrile. The samples were irradiated at 320 nm for 10 s. Concentration of the spin trap: 100 mM.

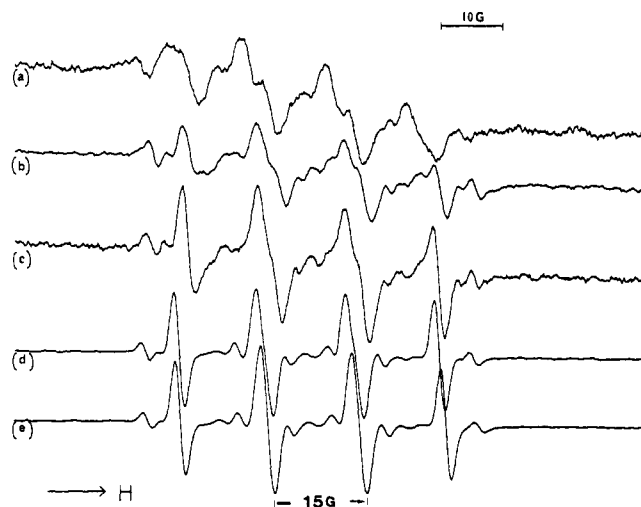


Figure 14. Effect of water on the ESR spectrum of the spin adduct of DMPO and the C/N-based radical formed in 1 mM solution of $[\text{Co}(\text{PMA})(\text{H}_2\text{O})](\text{ClO}_4)_2$ in oxygen-free acetonitrile plus 0% (trace a), 0.5% (trace b), 2% (trace c), 20% (trace d), and 40% (trace e) water. The samples were irradiated at 320 nm for 20 min. Concentration of spin trap: 100 mM.

radical in the presence of water has been proved in the present study. As seen in Figure 14, increasing amount of water in the solution of $[\text{Co}(\text{PMA})(\text{H}_2\text{O})](\text{ClO}_4)_2$ in acetonitrile under photolysis converts the eight-line spectrum into the typical four-line spectrum of the DMPO-OH spin adduct. Water, therefore, appears to exert a leveling effect in the sense that only $\cdot\text{OH}$ radical could be detected in the photolyzed aqueous solutions of 5-7. In contrast, the C/N-based radical formed with $[\text{Co}(\text{His})_2]\text{ClO}_4$ in oxygen-free acetonitrile is quite stable and is also detected in aqueous solution. As a result, $[\text{Co}(\text{His})_2]\text{ClO}_4$ induces minor damage to DNA under our experimental conditions.

Photolysis of free PMAH ligand in degassed aqueous buffer affords a very weak six-line ESR signal which is typical of the DMPO adducts of C-based radicals. No ESR signal from the DMPO-OH spin adduct is observed in this system. Clearly, coordination to cobalt(III) center facilitates the process of ligand reduction in 5-7, a process that leads to the production of $\cdot\text{OH}$ radical via the reaction of a C/N-based radical intermediate with water. Ligand of PMAH to the cobalt(III) center, therefore, appears to be the key to the formation of the C/N-based radical which eventually generates $\cdot\text{OH}$ radical in aqueous medium.

(78) Two facts, (i) no photoreduction was detected by analytical procedure and (ii) superoxide dismutase (SOD) exerts no effect on the DNA cleavage reactions by 5-7 (and Co(III)-BLMs), assert that $\cdot\text{OH}$ radicals are not produced by a Haber-Weiss type of reaction in the present cases.

(79) Peak, M. J.; Ito, A.; Foote, C. S.; Peak, J. G. *Photochem. Photobiol.* 1988, 47, 809. (b) Hoebeke, M.; Gandin, E.; Lion, Y. *Photochem. Photobiol.* 1986, 44, 543. (c) Mossoba, M. M.; Gutierrez, P. L. *Biochem. Biophys. Res. Commun.* 1985, 132, 445. (d) Chignell, C. F.; Kalyanaraman, B.; Sik, R. H.; Mason, R. P. *Photochem. Photobiol.* 1981, 34, 147.

(80) Diaziquone, 2,5-diaziridinyl-3,6-bis(carboethoxyamine)-1,4-benzoquinone was received as a gift from Dr. P. L. Gutierrez. For more information, see: Mossoba, M. M.; Gutierrez, P. L. *Biochem. Biophys. Res. Commun.* 1985, 132, 445.

Taken together, results of the DNA strand scission reactions and the spin-trapping experiments suggest the following mechanism for the observed DNA cleavage activity of 5-7. Because of the overall positive charge, these complexes stay very close to the DNA backbone in solution. Upon UV illumination, a C/N-based radical is formed on the ligand framework with the unpaired electron most possibly localized on the heterocyclic rings.⁸¹ This radical is unstable (detected by spin-trapping only in oxygen-free nonaqueous media) and rapidly reacts with water molecules to produce the $\cdot\text{OH}$ radical in close proximity of the DNA helix. Though many $\cdot\text{OH}$ radicals formed at this step diffuse into the bulk solution (and detected by spin-trapping), close association between the complexes and DNA allows a significant number of $\cdot\text{OH}$ radical to attack DNA and cause strand scission before the radicals escape the first hydration sphere. The importance of the proximity factor is clearly elucidated by the Na_2SO_4 experiment (Figure 9A). Since only the freely diffusible fraction of $\cdot\text{OH}$ radicals is quenched by radical scavengers like mannitol, these reagents have little effect on the photoinduced DNA cleavage activity of 5-7. This mechanism does not require dioxygen at any step. Indeed, dissolved oxygen acts as a radical scavenger in the DNA cleavage reactions, and this explains why more photocleavage is observed under anaerobic conditions (Figure S1). Modest variations in the extent of DNA damage by 5-7 could be related to differences in (a) the degree of stabilization and (b) the ease of formation of the C/N-based radical with different sixth ligands.

The same mechanism could account for the light-driven DNA cleavage capacity of the Co(III)-BLMs. Since PMAH closely resembles the metal-binding locus of BLM, it is quite possible that irradiation leads to the formation of a C/N-based radical in that portion of BLM in Co(III)-BLMs. Reaction of this unstable radical with water will then lead to the formation of $\cdot\text{OH}$ radical in the vicinity of the DNA strands. Presence of additional functionalities in BLM is supposed to hold and stabilize the $\cdot\text{OH}$ radical.⁸² Both GREEN and BROWN Co(III)-BLMs bind DNA strongly and hence will inflict significant damage to DNA through $\cdot\text{OH}$ radical-initiated reactions.⁸³ It is interesting to note that ORANGE Co(III)-BLM, which binds DNA less strongly,¹⁶ is also the one that causes the least damage to DNA. Overall, this mechanism of DNA damage by Co(III)-BLMs does not require dioxygen. It also explains why radical scavengers have little effect on the DNA cleavage reactions by Co(III)-BLMs.¹⁶

At this time, the above-mentioned mechanism is proposed as a plausible one for the photocleavage of DNA by Co(III)-BLMs. Results of several experiments support this mechanism. Nevertheless, more studies are required to elucidate the exact nature of the C/N-based radical.⁸⁴ Also, the kinetics of the photochemical reactions have to be determined. Such studies are in progress, and the results will be reported elsewhere.

Summary

The following are the principal results and conclusions of this investigation.

(81) For a recent review on formation of radicals (light-induced) on unsaturated nitrogen ligands in transition metal complexes, see: Kaim, W.; Deussner, B. O. In *Organometallic Radical Processes*; Elsevier: Amsterdam, 1990; Chapter 6.

(82) (a) Kittaka, A.; Sugano, Y.; Otsuka, M.; Ohno, M. *Tetrahedron* **1988**, *44*, 2811. (b) Kenani, A.; Bailly, C.; Helbecque, N.; Catteau, J.-P.; Houssin, R.; Bernier, J.-L.; Henichart, J.-P. *Biochem. J.* **1988**, *253*, 497. (c) Kittaka, A.; Sugano, Y.; Otsuka, M.; Ohno, M.; Sugiura, Y.; Umezawa, H. *Tetrahedron Lett.* **1986**, *27*, 3631, 3635.

(83) The sequence specificity observed in the photocleavage reactions by Co(III)-BLMs¹⁶ is very similar to that observed in the O_2 -dependent DNA cleavage reaction of Fe-BLM and could very well be related to the way the BLM complexes bind to DNA at the initial stage.

(84) Experiments to determine the spectral parameters of the C/N-based radical with the aid of time-resolved laser spectroscopy are in progress in this laboratory.

(i) Three cobalt(III) complexes 5-7 of a designed ligand PMAH that mimics the metal-chelating domain of the antitumor antibiotic bleomycin have been synthesized and structurally characterized. In these complexes, the uninegative PMA^- ligand (the peptide group gets deprotonated) employs five nitrogen donors located in the primary and secondary amines, pyrimidine and imidazole rings, and the amide moiety to bind cobalt(III). The sixth ligand in these octahedral complexes (H_2O , N-MeIm , and Cl^- , respectively) has been varied to obtain three analogues that match the colors of the three reported Co(III)-BLMs (BROWN, ORANGE, and GREEN, respectively).

(ii) Similarities in spectral parameters between the analogues (5-7) and the respective Co(III)-BLMs suggest that BLM utilizes the pyrimidine ring as well as the β -aminoalanine and the β -hydroxy histidine moieties to bind cobalt in Co(III)-BLMs. In addition, H_2O is the sixth ligand on cobalt in BROWN Co(III)-BLM, while in ORANGE Co(III)-BLM, another N donor from the remaining portion of the drug is coordinated to the cobalt. Though GREEN Co(III)-BLM is reported to contain a hydroperoxy ($-\text{OOH}$) group on cobalt, 7 has Cl^- as the sixth ligand on the metal.⁸⁵ Nevertheless, spectroscopic (and other) properties of 7 mimic those of GREEN Co(III)-BLM very closely.

(iii) Like Co(III)-BLMs, the analogues 5-7 induce DNA strand breaks upon UV illumination. Characteristics of the DNA cleavage reaction by 5-7 parallel those reported for the analogous reaction by Co(III)-BLMs. For example, DNA degradation by 5-7 (and the Co(III)-BLMs) does not require dioxygen. Also, the cleavage capacity increases in the order $6 > 5 > 7$ much like the respective Co(III)-BLMs (Figure S2).

(iv) The DNA cleavage reaction by 5-7 is not initiated by singlet oxygen or Co^{2+} ions generated in solution as a result of photoreduction of the cobalt(III) complexes.

(v) Spin-trapping experiments with 5-7 (and Co(III)-BLMs) in DNA buffers demonstrate the production of $\cdot\text{OH}$ radical upon irradiation. The extent of DNA damage by the analogues correlate well with the concentration of $\cdot\text{OH}$ radical produced in such solutions. In contrast, photolysis in oxygen-free nonaqueous media gives rise to a C/N-based radical. This C/N-based radical rapidly reacts with water to product $\cdot\text{OH}$ radical.

(vi) Collectively, these results confirm that reaction between water and a C/N-based radical formed in the ligand framework of 5-7 upon illumination results in rapid production of $\cdot\text{OH}$ radical in close proximity of the DNA helix. This leads to rapid DNA damage.

(vii) The same mechanism could account for the photocleavage of DNA by Co(III)-BLMs.

Acknowledgment. Financial support from the American Cancer Society (CH-481) and the National Institutes of Health (CA 53076-01) is gratefully acknowledged.

Supplementary Material Available: Figure S1 showing comparison of the extent of DNA cleavage with 5 under anaerobic vs aerobic conditions; Figure S2 showing the different extents of DNA cleavage with the three complexes 5-7; crystal structural data for 5-7 including atomic coordinates and isotropic thermal parameters (Tables S1-S3), complete lists of bond distances (Tables S4-S6) and angles (Tables S7-S9), anisotropic thermal parameters (Tables S10-S12), and H-atom coordinates (Tables S13-S15) (18 pages); tables of observed and calculated structure factors (Tables S16-S18) (52 pages). Ordering information is given on any current masthead page.

(85) One of the reviewers has pointed out that GREEN Co(III)-BLM can be prepared in the absence of Cl^- . Complex 7 may therefore be considered to be a model for GREEN Co(III)-BLM in that, of all the three complexes in the two systems (PMAH and BLM), both 7 and Co(III)-BLM each contain the weakest ligand (Cl^- and HOO^- , respectively) in the first coordination sphere around cobalt.